

1 Estimation of Non-null SNP Effect Size Distributions Enables 2 the Detection of Enriched Genes Underlying Complex Traits

3
4 Wei Cheng^{1,2}, Sohini Ramachandran^{1,2†}, and Lorin Crawford^{2-4†}

5 **1 Department of Ecology and Evolutionary Biology, Brown University, Providence, RI,
6 USA**

7 **2 Center for Computational Molecular Biology, Brown University, Providence, RI, USA**

8 **3 Department of Biostatistics, Brown University, Providence, RI, USA**

9 **4 Center for Statistical Sciences, Brown University, Providence, RI, USA**

10 † Corresponding E-mail: sramachandran@brown.edu; lorin_crawford@brown.edu

11 Abstract

12 Traditional univariate genome-wide association studies generate false positives and negatives due to
13 difficulties distinguishing associated variants from variants with spurious nonzero effects that do not
14 directly influence the trait. Recent efforts have been directed at identifying genes or signaling pathways
15 enriched for mutations in quantitative traits or case-control studies, but these can be computationally
16 costly and hampered by strict model assumptions. Here, we present gene- ε , a new approach for identifying
17 statistical associations between sets of variants and quantitative traits. Our key insight is that enrichment
18 studies on the gene-level are improved when we reformulate the genome-wide SNP-level null hypothesis
19 to identify spurious small-to-intermediate SNP effects and classify them as non-causal. gene- ε efficiently
20 identifies enriched genes under a variety of simulated genetic architectures, achieving greater than a 90%
21 true positive rate at 1% false positive rate for polygenic traits. Lastly, we apply gene- ε to summary
22 statistics derived from six quantitative traits using European-ancestry individuals in the UK Biobank,
23 and identify enriched genes that are in biologically relevant pathways.

24 Author Summary

25 Enrichment tests augment the standard univariate genome-wide association (GWA) framework by identi-
26 fying groups of biologically interacting mutations that are enriched for associations with a trait of interest,
27 beyond what is expected by chance. These analyses model local linkage disequilibrium (LD), allow many
28 different mutations to be disease-causing across patients, and generate biologically interpretable hypothe-
29 ses for disease mechanisms. However, existing enrichment analyses are hampered by high computational
30 costs, and rely on GWA summary statistics despite the high false positive rate of the standard univariate
31 GWA framework. Here, we present the gene-level association framework gene- ε (pronounced “genie”),
32 an empirical Bayesian approach for identifying statistical associations between sets of mutations and
33 quantitative traits. The central innovation of gene- ε is reformulating the GWA null model to distinguish
34 between (i) mutations that are statistically associated with the disease but are unlikely to directly in-
35 fluence it, and (ii) mutations that are most strongly associated with a disease of interest. We find that,
36 with our reformulated SNP-level null hypothesis, our gene-level enrichment model outperforms existing
37 enrichment methods in simulation studies and scales well for application to emerging biobank datasets.
38 We apply gene- ε to six quantitative traits in the UK Biobank and recover novel and functionally validated
39 gene-level associations.

40 Introduction

41 Over the last decade, there has been an evolving debate about the types of insight genome-wide single-
42 nucleotide polymorphism (SNP) genotype data offer into the genetic architecture of complex traits [1–5].
43 In the traditional genome-wide association (GWA) framework, individual SNPs are tested independently
44 for association with a trait of interest. While this approach can have drawbacks [2, 3, 6], more recent
45 approaches that combine SNPs within a region have gained power to detect biologically relevant genes
46 and pathways enriched for correlations with complex traits [7–14]. Reconciling these two observations is
47 crucial for biomedical genomics.

48 In the traditional GWA model, each SNP is assumed to either (i) directly influence (or perfectly tag a
49 variant that directly influences) the trait of interest; or (ii) have no effect on the trait at all (see Fig. 1A).
50 Throughout this manuscript, for simplicity, we refer to SNPs under the former as “associated” and those
51 under latter as “non-associated”. These classifications are based on ordinary least squares (OLS) effect
52 size estimates for each SNP in a regression framework, where the null hypothesis assumes that the true
53 effects of non-associated SNPs are zero ($H_0: \beta_j = 0$). The traditional GWA model is agnostic to trait
54 architecture, and is underpowered with a high false-positive rate for “polygenic” traits or traits which
55 are generated by many mutations of small effect [5, 15–17].

56 Suppose that in truth each SNP in a GWA dataset instead belongs to one of *three* categories depending
57 on the underlying distribution of their effects on the trait of interest: (i) associated SNPs; (ii) non-
58 associated SNPs that emit spurious nonzero statistical signals; and (iii) non-associated SNPs with zero-
59 effects (Fig. 1B) [18]. Associated SNPs may lie in enriched genes that directly influence the trait of
60 interest. The phenomenon of a non-associated SNP emitting nonzero statistical signal can occur due
61 to multiple reasons. For example, spurious nonzero SNP effects can be due to some varying degree of
62 linkage disequilibrium (LD) with associated SNPs [19]; or alternatively, non-associated SNPs can have a
63 trans-interaction effect with SNPs located within an enriched gene. In either setting, spurious SNPs can
64 emit small-to-intermediate statistical noise (in some cases, even appearing indistinguishable from truly
65 associated SNPs), thereby confounding traditional GWA tests (Fig. 1B). Hereafter, we refer to this noise
66 as “epsilon-genic effects” (denoted in shorthand as “ ε -genic effects”). There is a need for a computational
67 framework that has the ability to identify mutations associated with a wide range of traits, regardless of
68 whether narrow-sense heritability is sparsely or uniformly distributed across the genome.

69 Here, we develop a new and scalable quantitative approach for testing aggregated sets of SNP-level
70 GWA summary statistics for enrichment of associated mutations in a given quantitative trait. In practice,
71 our approach can be applied to any user-specified set of genomic regions, such as regulatory elements,
72 intergenic regions, or gene sets. In this study, for simplicity, we refer to our method as a gene-level
73 test (i.e., an annotated collection of SNPs within the boundary of a gene). The key contribution of
74 our approach is that gene-level association tests should treat spurious SNPs with ε -genic effects as non-
75 associated variants. Conceptually, this requires assessing whether SNPs explain more than some “epsilon”
76 proportion of the phenotypic variance. In this generalized model, we reformulate the GWA null hypothesis
77 to assume *approximately* no association for spurious non-associated SNPs where

$$78 \quad H_0: \beta_j \approx 0, \quad \beta_j \sim \mathcal{N}(0, \sigma_\varepsilon^2), \quad j = 1, \dots, J \text{ SNPs.}$$

79 Here, σ_ε^2 denotes a “SNP-level null threshold” and represents the maximum proportion of phenotypic
80 variance explained (PVE) that is contributed by spurious non-associated SNPs. This null hypothesis
81 can be equivalently restated as $H_0: \mathbb{E}[\beta_j^2] \leq \sigma_\varepsilon^2$ (Fig. 1B). Non-enriched genes are then defined as genes
82 that only contain SNPs with ε -genic effects (i.e., $0 \leq \mathbb{E}[\beta_j^2] \leq \sigma_\varepsilon^2$ for every j -th SNP within that region).
83 Enriched genes, on the other hand, are genes that contain at least one associated SNP (i.e., $\mathbb{E}[\beta_j^2] > \sigma_\varepsilon^2$
84 for at least one SNP j within that region). By accounting for the presence of spurious ε -genic effects (i.e.,
85 through different values of σ_ε^2 which the user can subjectively control), our approach flexibly constructs
86 an appropriate GWA SNP-level null hypothesis for a wide range of traits with genetic architectures that
87 land anywhere on the polygenic spectrum (see Materials and Methods).

88 We refer to our gene-level association framework as “gene- ε ” (pronounced “genie”). gene- ε leverages
89 our modified SNP-level null hypothesis to lower false positive rates and increases power for identifying
90 gene-level enrichment within GWA studies. This happens via two key conceptual insights. First, gene-
91 ε regularizes observed (and inflated) GWA summary statistics so that SNP-level effect size estimates
92 are positively correlated with the assumed generative model of complex traits. Second, it examines the
93 distribution of regularized effect sizes to offer the user choices for an appropriate SNP-level null threshold
94 σ_ε^2 to distinguish associated SNPs from spurious non-associated SNPs. This makes for an improved
95 and refined hypothesis testing strategy for identifying enriched genes underlying complex traits. With
96 detailed simulations, we assess the power of gene- ε to identify significant genes under a variety of genetic
97 architectures, and compare its performance against multiple competing approaches [7, 10, 12, 14, 20]. We
98 also apply gene- ε to the SNP-level summary statistics of six quantitative traits assayed in individuals of
99 European ancestry from the UK Biobank [21].

100 Results

101 Overview of gene- ε

102 The gene- ε framework requires two inputs: GWA SNP-level effect size estimates, and an empirical linkage
103 disequilibrium (LD, or variance-covariance) matrix. The LD matrix can be estimated directly from
104 genotype data, or from an ancestry-matched set of samples if genotype data are not available to the
105 user. We use these inputs to both estimate gene-level contributions to narrow-sense heritability h^2 , and
106 perform gene-level enrichment tests. After preparing the input data, there are three steps implemented
107 in gene- ε , which are detailed below (Fig. 2).

108 First, we shrink the observed GWA effect size estimates via regularized regression (Figs. 2A and
109 B; Eq. (4) in Materials and Methods). This shrinkage step reduces the inflation of OLS effect sizes
110 for spurious SNPs [22], and increases their correlation with the assumed generative model for the trait
111 of interest (particularly for traits with high heritability; Fig. S1). When assessing the performance of
112 gene- ε in simulations, we considered different types of regularization for the effect size estimates: the
113 Least Absolute Shrinkage And Selection Operator (gene- ε -LASSO) [23], the Elastic Net solution (gene-
114 ε -EN) [24], and Ridge Regression (gene- ε -RR) [25]. We also assessed our framework using the observed
115 ordinary least squares (OLS) estimates without any shrinkage (gene- ε -OLS) to serve as motivation for
116 having regularization as a step in the framework.

117 Second, we fit a K -mixture Gaussian model to all regularized effect sizes genome-wide with the goal
118 of classifying SNPs as associated, non-associated with spurious statistical signal, or non-associated with
119 zero-effects (Figs. 1B and 2C; see also [18]). Each successive Gaussian mixture component has distinctly
120 smaller variances ($\sigma_1^2 > \dots > \sigma_K^2$) with the K -th component fixed at $\sigma_K^2 = 0$. Estimating these variance
121 components helps determine an appropriate k -th category to serve as the cutoff for SNPs with null effects
122 (i.e., choosing some variance component σ_k^2 to be the null threshold σ_ε^2). The gene- ε software allows users
123 to determine this cutoff subjectively. Intuitively, enriched genes are likely to contain important variants
124 with relatively larger effects that are categorized in the early-to-middle mixture components. Since the
125 biological interpretation of the middle components may not be consistent across trait architectures, we
126 take a conservative approach in our selection of a cutoff when determining associated SNPs. Without loss
127 of generality, we assume non-null SNPs appear in the first mixture component with the largest variance,
128 while null SNPs appear in the latter components. By this definition, non-associated SNPs with spurious
129 ε -genic or zero-effects then have PVEs that fall at or below the variance of the second component (i.e.,
130 $\sigma_\varepsilon^2 = \sigma_2^2$ and $H_0: \mathbb{E}[\beta_j^2] \leq \sigma_2^2$ for the j -th SNP). gene- ε allows for flexibility in the number of Gaussians
131 that specify the range of null and non-null SNP effects. To achieve genome-wide scalability, we estimate
132 parameters of the K -mixture model using an expectation-maximization (EM) algorithm.

133 Third, we group the regularized GWA summary statistics according to gene boundaries (or user-

134 specified SNP-sets) and compute a gene-level enrichment statistic based on a commonly used quadratic
135 form (Fig. 2D) [7, 12, 20]. In expectation, these test statistics can be naturally interpreted as the contri-
136 bution of each gene to the narrow-sense heritability. We use Imhof’s method [26] to derive a P -value for
137 assessing evidence in support of an association between a given gene and the trait of interest. Details for
138 each of these steps can be found in Materials and Methods, as well as in Supporting Information.

139 Performance Comparisons in Simulation Studies

140 To assess the performance of gene- ε , we simulated complex traits under multiple genetic architectures
141 using real genotype data on chromosome 1 from individuals of European ancestry in the UK Biobank
142 (Materials and Methods). Following quality control procedures, our simulations included 36,518 SNPs
143 (Supporting Information). Next, we used the NCBI’s Reference Sequence (RefSeq) database in the
144 UCSC Genome Browser [27] to annotate SNPs with the appropriate genes. Simulations were conducted
145 using two different SNP-to-gene assignments. In the first, we directly used the UCSC annotations which
146 resulted in 1,408 genes to be used in the simulation study. In the second, we augmented the UCSC gene
147 boundaries to include SNPs within ± 50 kb, which resulted in 1,916 genes in the simulation study. For both
148 cases, we assumed a linear additive model for quantitative traits, while varying the following parameters:
149 sample size ($N = 5,000$ or $10,000$); narrow-sense heritability ($h^2 = 0.2$ or 0.6); and the percentage of
150 enriched genes (set to 1% or 10%). In each scenario, we considered traits being generated with and
151 without additional population structure. In the latter setting, traits are simulated while also using the
152 top ten principal components of the genotype matrix as covariates to create stratification. Regardless of
153 the setting, GWA summary statistics were computed by fitting a single-SNP univariate linear model (via
154 OLS) without any control for population structure. Comparisons were based on 100 different simulated
155 runs for each parameter combination.

156 We compared the performance of gene- ε against that of five competing gene-level association or
157 enrichment methods: SKAT [20], VEGAS [7], MAGMA [10], PEGASUS [12], and RSS [14] (Supporting
158 Information). As previously noted, we also explored the performance of gene- ε while using various degrees
159 of regularization on effect size estimates, with gene- ε -OLS being treated as a baseline. SKAT, VEGAS,
160 and PEGASUS are frequentist approaches, in which SNP-level GWA P -values are drawn from a correlated
161 chi-squared distribution with covariance estimated using an empirical LD matrix [28]. MAGMA is also a
162 frequentist approach in which gene-level P -values are derived from distributions of SNP-level effect sizes
163 using an F -test [10]. RSS is a Bayesian model-based enrichment method which places a likelihood on
164 the observed SNP-level GWA effect sizes (using their standard errors and LD estimates), and assumes
165 a spike-and-slab shrinkage prior on the true SNP effects [29]. Conceptually, SKAT, MAGMA, VEGAS,
166 and PEGASUS assume null models under the traditional GWA framework, while RSS and gene- ε allow
167 for traits to have architectures with more complex SNP effect size distributions.

168 For all methods, we assess the power and false discovery rates (FDR) for identifying correct genes
169 at a Bonferroni-corrected threshold ($P = 0.05/1408$ genes = 3.55×10^{-5} and $P = 0.05/1916$ genes =
170 2.61×10^{-5} , depending on if the ± 50 kb buffer was used) or median probability model (posterior enrichment
171 probability > 0.5 ; see [30]) (Tables S1-S16). We also compare their ability to rank true positives over
172 false positives via receiver operating characteristic (ROC) and precision-recall curves (Figs. 3 and S2-S16).
173 While we find gene- ε and RSS have the best tradeoff between true and false positive rates, RSS does
174 not scale well for genome-wide analyses (Table 1). In many settings, gene- ε has similar power to RSS
175 (while maintaining a considerably lower FDR), and generally outperforms RSS in precision-versus-recall.
176 gene- ε also stands out as the best approach in scenarios where the observed OLS summary statistics
177 were produced without first controlling for confounding stratification effects in more heritable traits (i.e.,
178 $h^2 = 0.6$). Computationally, gene- ε gains speed by directly assessing evidence for rejecting the gene-level
179 null hypothesis, whereas RSS must compute the posterior probability of being an enriched gene (which
180 can suffer from convergence issues; Supporting Information). For context, an analysis of just 1,000 genes
181 takes gene- ε an average of 140 seconds to run on a personal laptop, while RSS takes around 9,400 seconds

182 to complete.

183 When using GWA summary statistics to identify genotype-phenotype associations, modeling the ap-
184 propriate trait architecture is crucial. As expected, all methods we compared in this study have relatively
185 more power for traits with high h^2 . However, our simulation studies confirm the expectation that the
186 max utility for methods assuming the traditional GWA framework (i.e., SKAT, MAGMA, VEGAS, and
187 PEGASUS) is limited to scenarios where heritability is low, phenotypic variance is dominated by just a
188 few enriched genes with large effects, and summary statistics are not confounded by population structure
189 (Figs. S2, S3, S9, and S10). RSS, gene- ε -EN, and gene- ε -LASSO robustly outperform these methods
190 for the other trait architectures (Figs. 3, S4-S8, and S11-S16). One major reason for this result is that
191 shrinkage and penalized regression methods appropriately correct for inflation in GWA summary statis-
192 tics (Fig. S1). For example, we find that the regularization used by gene- ε -EN and gene- ε -LASSO is able
193 to recover effect size estimates that are almost perfectly correlated ($r^2 > 0.9$) with the true effect sizes
194 used to simulate sparse architectures (e.g., simulations with 1% enriched genes). In Figs. S17-S24, we
195 show a direct comparison between gene- ε with and without regularization to show how inflated SNP-level
196 summary statistics directly affect the ability to identify enriched genes across different trait architectures.
197 Regularization also allows gene- ε to preserve type 1 error when traits are generated under the null hy-
198 pothesis of no gene enrichment. Importantly, our method is relatively conservative when GWA summary
199 statistics are less precise and derived from studies with smaller sample sizes (e.g., $N = 5,000$; Table S17).

200 Characterizing Genetic Architecture of Quantitative Traits in the UK Biobank

201 We applied gene- ε to 1,070,306 genome-wide SNPs and six quantitative traits — height, body mass index
202 (BMI), mean red blood cell volume (MCV), mean platelet volume (MPV), platelet count (PLC), waist-
203 hip ratio (WHR) — assayed in 349,414 European-ancestry individuals in the UK Biobank (Supporting
204 Information) [21]. After quality control, we regressed the top ten principal components of the genotype
205 data onto each trait to control for population structure, and then we derived OLS SNP-level effect
206 sizes using the traditional GWA framework. For completeness, we then analyzed these GWA effect size
207 estimates with the four different implementations of gene- ε . In the main text, we highlight results under
208 the Elastic Net solution; detailed findings with the other gene- ε approaches can be found in Supporting
209 Information.

210 While estimating ε -genetic effects, gene- ε provides insight into to the genetic architecture of a trait (Ta-
211 ble S18). For example, past studies have shown human height to have a higher narrow-sense heritability
212 (estimates ranging from 45-80%; [6, 31–39]). Using Elastic Net regularized effect sizes, gene- ε estimated
213 approximately 11% of SNPs in the UK Biobank to be statistically associated with height. This meant
214 approximately 110,000 SNPs had marginal PVEs $\mathbb{E}[\beta_j^2] > 0$ (Materials and Methods). This number is
215 similar to the 93,000 and 100,000 height associated variants previously estimated by Goldstein [40] and
216 Boyle et al. [4], respectively. Additionally, gene- ε identified approximately 2% of SNPs to be “causal”
217 (meaning they had PVEs greater than the SNP-level null threshold, $\mathbb{E}[\beta_j^2] > \sigma_2^2$); again similar to the
218 Boyle et al. [4] estimate of 3.8% causal SNPs for height using data from the GIANT Consortium [32],
219 and the Lello et al. [41] estimate of 3.1% causal SNPs for height using European-ancestry individuals in
220 the UK Biobank.

221 Compared to body height, narrow-sense heritability estimates for BMI have been considered both
222 high and low (estimates ranging from 25-60%; [31, 33, 34, 36, 37, 39, 42–45]). Such inconsistency is likely
223 due to difference in study design (e.g., twin, family, population-based studies), many of which have been
224 known to produce different levels of bias [44]. Here, our results suggest BMI to have a lower narrow-sense
225 heritability than height, with a slightly different distribution of null and non-null SNP effects. Specifically,
226 we found BMI to have 13% associated SNPs and 6% causal SNPs.

227 In general, we found our genetic architecture characterizations in the UK Biobank to reflect the same
228 general themes we saw in the simulation study. Less aggressive shrinkage approaches (e.g., OLS and
229 Ridge) are subject to misclassifications of associated, spurious, and non-associated SNPs. As a result,

230 these methods struggle to reproduce well-known narrow-sense heritability estimates from the literature,
231 across all six traits. This once again highlights the need for computational frameworks that are able to
232 appropriately correct for inflation in summary statistics.

233 gene- ϵ Identifies Refined List of Genetic Enrichments

234 Next, we applied gene- ϵ to the summary statistics from the UK Biobank and generated genome-wide
235 gene-level association P -values (panels A and B of Figs. 4 and S25-S29). As in the simulation study, we
236 conducted two separate analyses using two different SNP-to-gene annotations: (i) we used the RefSeq
237 database gene boundary definitions directly, or (b) we augmented the gene boundaries by adding SNPs
238 within a ± 50 kilobase (kb) buffer to account for possible regulatory elements. A total of 14,322 genes
239 were analyzed when using the UCSC boundaries as defined, and a total of 17,680 genes were analyzed
240 when including the 50kb buffer. The ultimate objective of gene- ϵ is to identify enriched genes, which we
241 define as containing at least one associated SNP and achieving a gene-level association P -value below a
242 Bonferroni-corrected significance threshold (in our two analyses, $P = 0.05/14322$ genes = 3.49×10^{-6} and
243 $P = 0.05/17680$ genes 2.83×10^{-6} , respectively; Tables S19-S24). As a validation step, we compared gene-
244 ϵ P -values to RSS posterior enrichment probabilities for each gene. We also used the gene set enrichment
245 analysis tool Enrichr [46] to identify dbGaP categories with an overrepresentation of significant genes
246 reported by gene- ϵ (panels C and D of Figs. 4 and S25-S29). A comparison of gene-level associations and
247 gene set enrichments between the different gene- ϵ approaches are also listed (Tables S25-S27).

248 Many of the candidate enriched genes we identified by applying gene- ϵ were not previously annotated
249 as having trait-specific associations in either dbGaP or the GWAS catalog (Fig. 4); however, many of these
250 same candidate genes have been identified by past publications as related to the phenotype of interest
251 (Table 2). It is worth noting that multiple genes would not have been identified by standard GWA
252 approaches since the top SNP in the annotated region had a marginal association below a genome-wide
253 threshold (see Table 2 and highlighted rows in Tables S19-S24). Additionally, 45% of the genes selected
254 by gene- ϵ were also selected by RSS. For example, gene- ϵ reports *C1orf150* as having a significant gene-
255 level association with MPV ($P = 1 \times 10^{-20}$ and RSS posterior enrichment probability of 1), which is
256 known to be associated with germinal center signaling and the differentiation of mature B cells that
257 mutually activate platelets [47–49]. Importantly, nearly all of the genes reported by gene- ϵ had evidence
258 of overrepresentation in gene set categories that were at least related to the trait of interest. As expected,
259 the top categories with Enrichr Q -values smaller than 0.05 for height and MPV were "Body Height" and
260 "Platelet Count", respectively. Even for the less heritable MCV, the top significant gene sets included
261 hematological categories such as "Transferrin", "Erythrocyte Indices", "Hematocrit", "Narcolepsy", and
262 "Iron" — all of which have verified and clinically relevant connections to trait [50–57].

263 Lastly, gene- ϵ also identified genes with rare causal variants. For example, *ZNF628* (which is not
264 mapped to height in the GWAS catalog) was detected by gene- ϵ with a significant P -value of 1×10^{-20}
265 (and $P = 4.58 \times 10^{-8}$ when the gene annotation included a 50kb buffer). Previous studies have shown a
266 rare variant *rs147110934* within this gene to significantly affect adult height [38]. Rare and low-frequency
267 variants are generally harder to detect under the traditional GWA framework. However, rare variants
268 have been shown to be important for explaining the variation of complex traits [28, 39, 58–61]. With
269 regularization and testing for spurious ϵ -genic effects, gene- ϵ is able to distinguish between rare variants
270 that are causal and SNPs with larger effect sizes due various types of correlations. This only enhances
271 the power of gene- ϵ to identify potential novel enriched genes.

272 Discussion

273 During the past decade, it has been repeatedly observed that the traditional GWA framework can struggle
274 to accurately differentiate between associated and spurious SNPs (which we define as SNPs that covary

275 with associated SNPs but do not directly influence the trait of interest). As a result, the traditional
276 GWA approach is prone to generating false positives, and detects variant-level associations spread widely
277 across the genome rather than aggregated sets in disease-relevant pathways [4]. While this observation
278 has spurred to many interesting lines of inquiry — such as investigating the role of rare variants in
279 generating complex traits [9, 28, 58, 59], comparing the efficacy of tagging causal variants in different
280 ancestries [62, 63], and integrating GWA data with functional -omics data [64–66] — the focus of GWA
281 studies and studies integrating GWA data with other -omics data is still largely based on the role of
282 individual variants, acting independently.

283 Here, our objective is to identify biologically significant underpinnings of the genetic architecture of
284 complex traits by modifying the traditional GWA null hypothesis from $H_0: \beta_j = 0$ (i.e., the j -th SNP
285 has zero statistical association with the trait of interest) to $H_0: \beta_j \approx 0$. We accomplish this by testing
286 for ε -genic effects: spurious small-to-intermediate effect sizes emitted by truly non-associated SNPs. We
287 use an empirical Bayesian approach to learn the effect size distributions of null and non-null SNP effects,
288 and then we aggregate (regularized) SNP-level association signals into a gene-level test statistic that
289 represents the gene’s contribution to the narrow-sense heritability of the trait of interest. Together, these
290 two steps reduce false positives and increase power to identify the mutations, genes, and pathways that
291 directly influence a trait’s genetic architecture. By considering different thresholds for what constitutes
292 a null SNP effect (i.e., different values of σ_ε^2 for spurious non-associated SNPs; Figs. 1 and 2), gene-
293 ε offers the flexibility to construct an appropriate null hypothesis for a wide range of traits with genetic
294 architectures that land anywhere on the polygenic spectrum. It is important to stress that while we
295 repeatedly point to our improved ability distinguish “causal” variants in enriched genes, gene- ε is by no
296 means a causal inference procedure. Instead, it is an association test which highlights genes in enriched
297 pathways that are most likely to be associated with the trait of interest.

298 Through simulations, we showed the gene- ε framework outperforms other widely used gene-level asso-
299 ciation methods (particularly for highly heritable traits), while also maintaining scalability for genome-
300 wide analyses (Figs. 3 and S2-S24, and Tables 1 and S1-17). Indeed, all the approaches we compared in
301 this study showed improved performance when they used summary statistics derived from studies with
302 larger sample sizes (i.e., simulations with $N = 10,000$). This is because the quality of summary statistics
303 also improves in these settings (via the asymptotic properties of OLS estimates). Nonetheless, our results
304 suggest that applying gene- ε to summary statistics from previously published studies will increase the
305 return made on investments in GWA studies over the last decade.

306 Like any aggregated SNP-set association method, gene- ε has its limitations. Perhaps the most obvi-
307 ous limitation is that annotations can bias the interpretation of results and lead to erroneous scientific
308 conclusions (i.e., might cause us to highlight the “wrong” gene [14, 67, 68]). We observed some instances
309 of this during the UK Biobank analyses. For example, when studying MPV, *CAPN10* only appeared
310 to be a significant gene after its UCSC annotated boundary was augmented by a ± 50 kb buffer win-
311 dow ($P = 1.85 \times 10^{-1}$ and $P = 1.17 \times 10^{-7}$ before and after the buffer was added, respectively; Table
312 S22). After further investigation, this result occurred because the augmented definition of *CAPN10*
313 included nearly all causal SNPs from the significant neighboring gene *RNPEPL1* ($P = 1 \times 10^{-20}$ and
314 $P = 2.07 \times 10^{-9}$ before and after the buffer window was added, respectively). While this shows the need
315 for careful biological interpretation of the results, it also highlights the power of gene- ε to prioritize true
316 genetic signal effectively.

317 Another limitation of gene- ε is that it relies on the user to determine an appropriate SNP-level null
318 threshold σ_ε^2 to serve as a cutoff between null and non-null SNP effects. In the current study, we use a
319 K -mixture Gaussian model to classify SNPs into different categories and then (without loss of generality)
320 we subjectively assume that associated SNPs only appear in the component with the largest variance
321 (i.e., we choose $\sigma_\varepsilon^2 = \sigma_2^2$). Indeed, there can be many scenarios where this particular threshold choice is
322 not optimal. For example, if there is one very strongly associated locus, the current implementation of
323 the algorithm will assign it to its own mixture component and all other SNPs will be assumed to be not

324 associated with the trait, regardless of the size of their corresponding variances. As previously mentioned,
325 one practical guideline would be to select σ_ε^2 based on some *a priori* knowledge about a trait's architecture.
326 However, a more robust approach would be to select the SNP-null hypothesis threshold based on the data
327 at hand. One way to do this would be to take a fully Bayesian approach and allow posterior inference
328 on σ_ε^2 to be dependent upon how much heritability is explained by SNPs placed in the top few largest
329 components of the normal mixture. Recently, sparse Bayesian parametric [69] and nonparametric [70]
330 Gaussian mixture models have been proposed for improved polygenic prediction with summary statistics.
331 Combining these modeling strategies with our modified SNP-level null hypothesis could make for a more
332 unified and data-driven implementation of the gene- ε framework.

333 There are several other potential extensions for the gene- ε framework. First, in the current study,
334 we only focused on applying gene- ε to quantitative traits (Figs. 4 and S25-S29, and Tables 2 and S18-
335 S27). Future studies extending this approach to binary traits (e.g., case-control studies) should explore
336 controlling for additional confounders that can occur within these phenotypes, such as ascertainment
337 [71–73]. Second, we only focus on data consisting of common variants; however, it would be interesting
338 to extend gene- ε for (i) rare variant association testing and (ii) studies that consider the combined
339 effect between rare and common variants. A significant challenge, in either case, would be to adaptively
340 adjust the strength of the regularization penalty on the observed OLS summary statistics for causal rare
341 variants, so as to not misclassify them as spurious non-associated SNPs. Previous approaches with specific
342 re-weighting functions for rare variants may help here [9, 28, 58] (Materials and Methods). A final related
343 extension of gene- ε is to include information about standard errors when estimating ε -genic effects. In
344 our analyses using the UK Biobank, some of the newly identified candidate genes contained SNPs that
345 had large effect sizes but insignificant P -values in the original GWA analysis (after Bonferroni-correction;
346 Tables 2 and S19-S24). While this could be attributed to the modified SNP-level null distribution
347 assumed by gene- ε , it also motivates a regularization model that accounts for the standard error of effect
348 size estimates from GWA studies [14, 22, 29].

349 Acknowledgements

350 The authors would like to thank the Editor, Associate Editor, Doug Speed, and the other two anonymous
351 referees for their constructive comments. The authors also thank Xiang Zhu (Stanford University) for
352 help with the implementation of RSS, as well as Sam Smith (Brown University) for help with the man-
353 agement of the UK Biobank data. This research was conducted using the UK Biobank Resource under
354 Application Number 22419, and part of this research was conducted using computational resources and
355 services at the Center for Computation and Visualization (CCV), Brown University. S. Ramachandran
356 also acknowledges support from a Natural Sciences Fellowship at the Swedish Collegium for Advanced
357 Study (Spring 2019), and by the Erling-Persson Family Foundation and the Knut and Alice Wallenberg
358 Foundation.

359 Funding Sources

360 This research was supported in part by US National Institutes of Health (NIH) grant R01 GM118652 and
361 National Science Foundation (NSF) CAREER award DBI-1452622 to S. Ramachandran. This research
362 was also partly supported by grants P20GM109035 (COBRE Center for Computational Biology of Human
363 Disease; PI Rand) and P20GM103645 (COBRE Center for Central Nervous; PI Sanes) from the NIH
364 NIGMS, 2U10CA180794-06 from the NIH NCI and the Dana Farber Cancer Institute (PIs Gray and
365 Gatsonis), as well as by an Alfred P. Sloan Research Fellowship awarded to L. Crawford. Any opinions,
366 findings, and conclusions or recommendations expressed in this material are those of the authors and do
367 not necessarily reflect the views of any of the funders or supporters. The funders had no role in study

368 design, data collection and analysis, decision to publish, or preparation of the manuscript.

369 **Author Contributions**

370 W.C., S.R., and L.C. conceived the methods. W.C. developed the software and carried out all analyses.

371 W.C., S.R., and L.C. wrote and reviewed the manuscript.

372 **Competing Interests**

373 The authors declare no competing interests.

374 Materials and Methods

375 Traditional Association Tests using Summary Statistics

376 gene- ε requires two inputs: genome-wide association (GWA) marginal effect size estimates $\widehat{\beta}$, and an
 377 empirical linkage disequilibrium (LD) matrix Σ . We assumed the following generative linear model for
 378 complex traits

$$379 \quad \mathbf{y} = \mathbf{X}\boldsymbol{\beta} + \mathbf{e}, \quad \mathbf{e} \sim \mathcal{N}(\mathbf{0}, \tau^2\mathbf{I}), \quad (1)$$

380 where \mathbf{y} denotes an N -dimensional vector of phenotypic states for a quantitative trait of interest measured
 381 in N individuals; \mathbf{X} is an $N \times J$ matrix of genotypes, with J denoting the number of single nucleotide
 382 polymorphisms (SNPs) encoded as $\{0, 1, 2\}$ copies of a reference allele at each locus; $\boldsymbol{\beta}$ is a J -dimensional
 383 vector containing the additive effect sizes for an additional copy of the reference allele at each locus on \mathbf{y} ;
 384 \mathbf{e} is a normally distributed error term with mean zero and scaled variance τ^2 ; and \mathbf{I} is an $N \times N$ identity
 385 matrix. For convenience, we assumed that the genotype matrix (column-wise) and trait of interest have
 386 been mean-centered and standardized. We also treat $\boldsymbol{\beta}$ as a fixed effect. A central step in GWA studies is
 387 to infer $\boldsymbol{\beta}$ for each SNP, given both genotypic and phenotypic measurements for each individual sample.
 388 For every SNP j , gene- ε takes in the ordinary least squares (OLS) estimates based on Eq. (1)

$$389 \quad \widehat{\beta}_j = (\mathbf{x}_j^T \mathbf{x}_j)^{-1} \mathbf{x}_j^T \mathbf{y}, \quad (2)$$

390 where \mathbf{x}_j is the j -th column of the genotype matrix \mathbf{X} , and $\widehat{\beta}_j$ is the j -th entry of the vector $\widehat{\boldsymbol{\beta}}$. In
 391 traditional GWA studies, the null hypothesis for statistical association tests assumes $H_0: \beta_j = 0$ for all
 392 $j = 1, \dots, J$ SNPs. It can be shown that two genotypic variants \mathbf{x}_j and $\mathbf{x}_{j'}$ in linkage disequilibrium
 393 (LD) will produce effect size estimates $\widehat{\beta}_j$ and $\widehat{\beta}_{j'}$ ($j \neq j'$) that are correlated [29]. This can lead to
 394 confounded statistical tests. For the applications considered here, the LD matrix is empirically estimated
 395 from external data (e.g., directly from GWA study data, or using an LD map from a population with
 396 similar genomic ancestry to that of the samples analyzed in the GWA study).

397 Regularized Regression for GWA Summary Statistics

398 gene- ε uses regularization on the observed GWA summary statistics to reduce inflation of SNP-level
 399 effect size estimates and increase their correlation with the assumed generative model of complex traits.
 400 For large sample size N , note that the asymptotic relationship between the observed GWA effect size
 401 estimates $\widehat{\boldsymbol{\beta}}$ and the true coefficient values $\boldsymbol{\beta}$ is [18, 74, 75]

$$402 \quad \mathbb{E}[\widehat{\beta}_j] = \sum_{j'=1}^J \rho(\mathbf{x}_j, \mathbf{x}_{j'}) \beta_{j'} \quad \iff \quad \mathbb{E}[\widehat{\boldsymbol{\beta}}] = \Sigma \boldsymbol{\beta}, \quad (3)$$

403 where $\Sigma_{jj'} = \rho(\mathbf{x}_j, \mathbf{x}_{j'})$ denotes the correlation coefficient between SNPs \mathbf{x}_j and $\mathbf{x}_{j'}$. The above mirrors
 404 a high-dimensional regression model with the misestimated OLS summary statistics as the response
 405 variables and the LD matrix as the design matrix. Theoretically, the resulting output coefficients from
 406 this model are the desired true effect size estimates. Due to the multi-collinear structure of GWA data, we
 407 cannot reuse the ordinary least squares solution reliably [76]. Thus, we derive the general regularization

$$408 \quad \widetilde{\boldsymbol{\beta}} = \arg \min_{\boldsymbol{\beta}} \|\widehat{\boldsymbol{\beta}} - \Sigma \boldsymbol{\beta}\|^2, \quad \text{subject to } (1 - \alpha) \|\boldsymbol{\beta}\|_1 + \alpha \|\boldsymbol{\beta}\|_2^2 \leq t \text{ for some } t, \quad (4)$$

409 where, in addition to previous notation, the solution $\widetilde{\boldsymbol{\beta}}$ is used to denote the regularized solution of the
 410 observed GWA effect sizes $\widehat{\boldsymbol{\beta}}$; and $\|\boldsymbol{\cdot}\|_1$ and $\|\boldsymbol{\cdot}\|_2^2$ denote L_1 and L_2 penalties, respectively. The free
 411 regularization parameter t is chosen based off a grid $[\log t_{\min}, \log t_{\max}]$ with 100 sequential steps of size

412 0.01. Here, t_{\max} is the minimum value such that all summary statistics are shrunk to zero. We then
413 select the t that results in a model with an R^2 within one standard error of the best fitted model. In
414 other words, we choose the t that (i) results in a more sparse solution than the best fitted model, but
415 (ii) cannot be distinguished from the best fitted model in terms of overall variance explained.

416 The term α in Eq. (4) distinguishes the type of regularization used, and can be chosen to induce various
417 degrees of shrinkage on the effect size estimates. Specifically, $\alpha = 0$ corresponds to the “Least Absolute
418 Shrinkage and Selection Operator” or LASSO solution [23], $\alpha = 1$ equates to Ridge Regression [25],
419 while $0 < \alpha < 1$ results in the Elastic Net [24]. The LASSO solution forces some inflated coefficients
420 to be zero; while the Ridge shrinks the magnitudes of all coefficients but does not set any of them to
421 be exactly zero. Intuitively, the LASSO will create a regularized set of effect sizes where associated
422 SNPs have larger effects, non-associated SNPs with spurious small-to-intermediate (or ε -genic) effects,
423 and non-associated SNPs with zero-effects. It has been suggested that the L_1 -penalty can suffer from a
424 lack of stability [77]. Therefore, in the main text, we also highlighted gene- ε using the Elastic Net (with
425 $\alpha = 0.5$). The Elastic Net is a convex combination of the LASSO and Ridge penalties, but still produces
426 distinguishable sets of associated, spurious, and non-associated SNPs. Note that for large GWA studies
427 (e.g., the UK Biobank analysis in the main text), it can be impractical to construct a genome-wide LD
428 matrix; therefore, we regularize OLS effect size estimates based on partitioned chromosome specific LD
429 matrices. Results comparing each of the gene- ε regularization implementations are given in the main
430 text (Fig. 3) and Supporting Information (Figs. S2-S24 and Tables S1-18 and 25-27). We will describe
431 how we approximate the null distribution for these regularized GWA summary statistics over the next
432 two sections.

433 Estimating the SNP-Level Null Threshold

434 The main innovation of gene- ε is to treat spurious SNPs with ε -genic effects as non-associated. This
435 leads to reformulating the GWA SNP-level null hypothesis to assume non-associated SNPs can make
436 small-to-intermediate contributions to the phenotypic variance. Formally, we write this as

$$437 H_0: \beta_j \approx 0, \quad \beta_j \sim \mathcal{N}(0, \sigma_\varepsilon^2), \quad j = 1, \dots, J \quad (5)$$

438 where σ_ε^2 denotes the “SNP-level null threshold” and represents the maximum proportion of phenotypic
439 variance explained (PVE) that is contributed by spurious SNPs. Based on Eq. (5), we equivalently say

$$440 H_0: \mathbb{E}[\beta_j^2] \leq \sigma_\varepsilon^2. \quad (6)$$

441 To estimate the threshold σ_ε^2 for null SNP-level effects, we use an empirical Bayesian approach and fit a
442 K -mixture of normal distributions over the (regularized) effect size estimates [18],

$$443 \tilde{\beta}_j | z_j = k \sim \mathcal{N}(0, \sigma_k^2), \quad \Pr[z_j = k] = \pi_k, \quad (7)$$

444 where $z_j \in \{1, \dots, K\}$ is a latent variable representing the categorical membership for the j -th SNP.
445 When summing over all components, Eq. (7) corresponds to the following marginal distribution

$$446 \tilde{\beta}_j \sim \sum_{k=1}^K \pi_k \mathcal{N}(0, \sigma_k^2), \quad (8)$$

447 where π_k is a mixture weight representing the marginal (unconditional) probability that a randomly
448 selected SNP belongs to the k -th component, with $\sum_k \pi_k = 1$. The above mixture allows for distinct
449 clusters of nonzero effects through K different variance components (σ_k^2 , $k = 1, \dots, K$) [18]. Here, we
450 consider sequential fractions (π_1, \dots, π_K) of SNPs to correspond to distinctly smaller effects ($\sigma_1^2 > \dots >$
451 $\sigma_K^2 = 0$) [18]. The goal of the mixture model is to “bin” each of the (regularized) SNP-level effects

and determine an appropriate category k to serve as the cutoff for SNPs with null effects (i.e., choosing the threshold σ_ϵ^2 based on some σ_k^2). Such a threshold can be chosen based on *a priori* knowledge about the phenotype of interest. It is intuitive to assume that enriched genes will contain non-null SNPs that classify within the early-to-middle mixture components; unfortunately, the biological interpretations of the middle components may not be consistent across trait architectures. Therefore, without loss of generality in this paper, we take a conservative approach in our definition of associated SNPs within enriched genes. Here, we subjectively set the SNP-level null threshold as $\sigma_\epsilon^2 = \sigma_2^2$. Thus, non-null SNPs are assumed to appear in the largest fraction (i.e., the alternative $H_A: \mathbb{E}[\beta_j^2] > \sigma_2^2$), while null SNPs with belong to the latter groups (i.e., the null $H_0: \mathbb{E}[\beta_j^2] \leq \sigma_2^2$). Given Eqs. (7) and (8), we write the joint log-likelihood for all J SNPs as the following

$$\log p(\tilde{\boldsymbol{\beta}} | \boldsymbol{\Theta}) = \sum_{j=1}^J \log p(\tilde{\beta}_j | \boldsymbol{\Theta}) = \sum_{j=1}^J \log \left\{ \sum_{k=1}^K \pi_k \mathcal{N}(0, \sigma_k^2) \right\}, \quad (9)$$

where $\boldsymbol{\Theta} = (\pi_1, \dots, \pi_K, \sigma_1^2, \dots, \sigma_K^2)$ is the complete set of parameters for the mixture model. Since there is not a closed-form solution for the maximum likelihood estimate (MLE), so we use an expectation-maximization (EM) algorithm to estimate the parameters in $\boldsymbol{\Theta}$ [78–80].

Derivation of the EM Algorithm. To derive an EM solution, we use Eqs. (7) and (8) to write the joint distribution of the J -regularized SNP-level effect sizes and the J -latent random variables $\mathbf{z} = (z_1, \dots, z_J)$, conditioned on the mixture parameters $\boldsymbol{\Theta}$,

$$p(\tilde{\boldsymbol{\beta}}, \mathbf{z} | \boldsymbol{\Theta}) = p(\tilde{\boldsymbol{\beta}} | \mathbf{z}, \boldsymbol{\Theta}) p(\mathbf{z}) = \prod_{j=1}^J \prod_{k=1}^K [\pi_k \mathcal{N}(0, \sigma_k^2)]^{\mathbb{I}(z_j=k)}, \quad (10)$$

where $\mathbb{I}(z_j = k)$ is an indicator function and equates to one if $z_j = k$ and zero otherwise. Taking the log of this distribution yields the following

$$\log p(\tilde{\boldsymbol{\beta}}, \mathbf{z} | \boldsymbol{\Theta}) = \sum_{j=1}^J \log p(\tilde{\beta}_j, z_j | \boldsymbol{\Theta}) = \sum_{j=1}^J \sum_{k=1}^K \mathbb{I}(z_j = k) [\log \pi_k + \log \mathcal{N}(0, \sigma_k^2)]. \quad (11)$$

As opposed to Eq. (9), the augmented log-likelihood in Eq. (11) is a much simpler function for which to find a solution. The formal steps of the EM algorithm are now detailed below:

1. E-Step: Update the Probability of Fraction Assignment. In the E-step of the EM algorithm, we estimate the probability that the j -th SNP belongs to one of the K fraction groups. To begin, we use Bayes theorem to find

$$p(\mathbf{z} | \tilde{\boldsymbol{\beta}}, \boldsymbol{\Theta}) \propto p(\tilde{\boldsymbol{\beta}} | \mathbf{z}, \boldsymbol{\Theta}) p(\mathbf{z}) = \prod_{j=1}^J \prod_{k=1}^K [\pi_k \mathcal{N}(0, \sigma_k^2)]^{\mathbb{I}(z_j=k)}. \quad (12)$$

Next, we take the expectation of the complete log-likelihood $\log p(\tilde{\boldsymbol{\beta}}, \mathbf{z} | \boldsymbol{\Theta})$, with respect to the conditional distribution $p(\mathbf{z} | \tilde{\boldsymbol{\beta}}, \boldsymbol{\Theta})$, under current value of the mixture parameters $\hat{\boldsymbol{\Theta}}$. This yields

$$\mathbb{E}_{\mathbf{z} | \tilde{\boldsymbol{\beta}}, \hat{\boldsymbol{\Theta}}} [\log p(\tilde{\boldsymbol{\beta}}, \mathbf{z} | \hat{\boldsymbol{\Theta}})] = \sum_{j=1}^J \sum_{k=1}^K \hat{\gamma}_k^{(j)} [\log \pi_k + \log \mathcal{N}(0, \sigma_k^2)], \quad (13)$$

where $\hat{\gamma}_k^{(j)}$ is referred to as the “responsibility of the k -th mixture component”, and is given as

$$\hat{\gamma}_k^{(j)} = \Pr[z_j = k | \tilde{\beta}_j, \hat{\boldsymbol{\Theta}}] = \frac{\hat{\pi}_k \mathcal{N}(0, \hat{\sigma}_k^2)}{\sum_{k'=1}^K \hat{\pi}_{k'} \mathcal{N}(0, \hat{\sigma}_{k'}^2)}. \quad (14)$$

484 Intuitively, the EM algorithm uses the collection of these responsibility values to assign SNPs to
 485 one of the K fraction groups. This key step may be interpreted as determining the category of SNP
 486 effects (which is determined by identifying the k -th component with the largest $\gamma_k^{(j)}$ for each j -th
 487 SNP).

488 **2. M-Step: Update the Component Variances and Mixture Weights.** In the M-step of the
 489 EM algorithm, we now fix the responsibility values and maximize the expectation in Eq. (13), with
 490 respect to the parameters in $\hat{\Theta}$. Namely, we compute the following closed-form solutions:

$$491 \quad \hat{\sigma}_k^2 = \frac{1}{J_k} \sum_{j=1}^J \hat{\gamma}_k^{(j)} \tilde{\beta}_j^2, \quad \hat{\pi}_k = \frac{J_k}{J} \quad (15)$$

492 where $J_k = \sum_j \hat{\gamma}_k^{(j)}$ is the sum of the membership weights for the k -th mixture component and
 493 represents the number of SNPs assigned to that component. The $\hat{\sigma}_k^2$ estimates are used to set the
 494 SNP-level null threshold $\hat{\sigma}_\varepsilon^2$.

495 The gene- ε software implements the above EM algorithm using the `mclust` [81] package in R. Results in
 496 the main text and Supporting Information are based on 100 iterations from 10 different parallel chains
 497 to ensure convergence. To implement the above algorithm, we use the `mclust` software package which
 498 can fit a Gaussian mixture with up to $K = 10$ distinct components (see Software Details). Here, the
 499 function will compare the Bayesian Information Criterion (BIC) approximation to the Bayes factor for
 500 each possible K [82], and produces a resulting output for the K value that has the largest BIC value.
 501 Note that since the EM updates do not involve any large LD matrices, the algorithm scales to be fit
 502 efficiently over all SNPs genome-wide.

503 Regularized GWA Summary Statistics under the Null Hypothesis

504 With an estimate of the SNP-level null threshold σ_ε^2 , we now describe the probabilistic distribution
 505 of the regularized GWA summary statistics under the null hypothesis. Without loss of generality, we
 506 demonstrate this property using the general regularization approach where we fix $\alpha \in [0, 1]$ and have the
 507 following (approximate) closed form solution for the regularized effect size estimates [23–25]

$$508 \quad \tilde{\beta} \simeq \mathbf{H}\hat{\beta}, \quad \mathbf{H} = (\mathbf{\Sigma} + \vartheta\mathbf{D}^{-1})^{-1} \quad (16)$$

509 with $\vartheta \geq 0$ being a penalization parameter that has one-to-one correspondence with t in Eq. (4). Here, \mathbf{H} is
 510 commonly referred to as the “linear shrinkage estimator” [citation], where \mathbf{D} is a diagonal weight matrix
 511 with nonzero elements dictated by the type of regularization that is being used. For example, $\mathbf{D} = \mathbf{I}$ while
 512 performing ridge regression [25], and $\mathbf{D} = \text{diag}(|\tilde{\beta}_1|, \dots, |\tilde{\beta}_p|)$ while using ridge-based approximations for
 513 the elastic net and lasso solutions [23, 24]. From Eq. (16), it is clear that $\tilde{\beta}$ may be interpreted as
 514 a marginal estimator of SNP-level effects after accounting for LD structure. Using Eqs. (2)-(3), it is
 515 straightforward to show the (approximate) relationship between the regularized effect size estimates and
 516 the true coefficient values

$$517 \quad \mathbb{E}[\tilde{\beta}] \simeq \mathbf{H}\mathbf{\Sigma}\beta. \quad (17)$$

518 As described in the main text, the accuracy of this relationship is dependent upon both the sample size
 519 and narrow-sense heritability of the trait of interest (Fig. S1). Indeed, if $\mathbf{\Sigma}$ is full rank and regularization
 520 is no longer implemented (i.e., $\vartheta = 0$), $\tilde{\beta}$ is simply the ordinary least squares solution for marginal GWA
 521 summary statistics with asymptotic variance-covariance $\mathbb{V}[\tilde{\beta}] \simeq \mathbf{\Sigma}$ under the null model [18, 74, 75]. In the
 522 limiting case where the number of observations in a GWA study is large (i.e., $N \rightarrow \infty$) and the trait of
 523 interest is highly heritable, $\tilde{\beta}$ converges onto β in expectation; and thus is assumed to be independently

524 and normally distributed under the null hypothesis with asymptotic variance $\sigma_\varepsilon^2 \mathbf{I}$ (previously discussed
 525 in Eq. (5)). As empirically demonstrated for synthetic traits in the current study, we are rarely in
 526 situations where we expect the regularized effect size estimates to have completely converged onto the
 527 true generative SNP-level coefficients (again see Fig. S1). This effectively means that we cannot expect
 528 each $\tilde{\beta}_j$ to be completely independent under the null hypothesis in practice. We accommodate this
 529 realization by assuming that under the null model

$$530 \quad \mathbb{V}[\tilde{\boldsymbol{\beta}}] = \sigma_\varepsilon^2 \boldsymbol{\Sigma}, \quad \lim_{\sigma_\varepsilon^2 \rightarrow 0} \sigma_\varepsilon^2 \boldsymbol{\Sigma} = \sigma_\varepsilon^2 \mathbf{I} \quad (18)$$

531 Our reasoning for the formulation above is that, for most quality controlled studies, SNPs in perfect LD
 532 will have been pruned such that $\rho(\mathbf{x}_j, \mathbf{x}_{j'}) < \rho(\mathbf{x}_j, \mathbf{x}_j)$ for all $j \neq j'$ variants in the data. Therefore, when
 533 traits are generated under the idealized null scenario with large sample sizes and no genetic effects, the
 534 estimate of $\sigma_\varepsilon^2 \rightarrow 0$ and the off-diagonals of $\sigma_\varepsilon^2 \boldsymbol{\Sigma}$ will approach zero quicker than the diagonal elements;
 535 thus, allowing the regularized $\tilde{\boldsymbol{\beta}}$ to asymptotically converge onto the true coefficients $\boldsymbol{\beta}$. When this
 536 scenario does not occur, we are able to appropriately deal with the remaining correlation structure (e.g.,
 537 all the simulation scenarios explored in this work; see Figs. 3 and S2-S24, and Tables 1 and S1-17).

538 Using the SNP-Level Null Threshold to Detect Enriched Genes

539 We now formalize the hypothesis test for identifying significantly enriched genes conditioned on the
 540 SNP-level null threshold σ_ε^2 , which we compute using the variance component estimates from the EM
 541 algorithm detailed in the previous section. The gene- ε gene-level test statistic is based on a quadratic
 542 form using GWA summary statistics, which is a common approach for generating gene-level test statistics
 543 for complex traits. Let gene (or genomic region) g represent a known set of SNPs $j \in \mathcal{J}_g$; for example, \mathcal{J}_g
 544 may include SNPs within the boundaries of g and/or within its corresponding regulatory region. Here, we
 545 conformably partition the regularized GWA effect size estimates $\tilde{\boldsymbol{\beta}}$ and define the gene-level test statistic

$$546 \quad \tilde{Q}_g = \tilde{\boldsymbol{\beta}}_g^\top \mathbf{A} \tilde{\boldsymbol{\beta}}_g, \quad (19)$$

547 where \mathbf{A} is an arbitrary symmetric and positive semi-definite weight matrix. We set to $\mathbf{A} = \mathbf{I}$ to be
 548 the identity matrix for all analyses in the current study; hence, \tilde{Q}_g simplifies to a sum of squared SNP
 549 effects in the g -th gene. Indeed, similar quadratic forms have been implemented to assess the enrichment
 550 of mutations at the gene level [7, 12] and across general SNP-sets [9, 20, 28, 58]. A key feature of the
 551 gene- ε framework is to assess the statistics in Eq. (19) against a gene-level enrichment null hypothesis
 552 $H_0: Q_g = 0$ that is dependent on the SNP-level null threshold σ_ε^2 . Due to the normality assumption for
 553 each SNP effect in Eq. (5), Q_g is theoretically assumed to follow a mixture of chi-square distributions,

$$554 \quad Q_g \sim \sum_{j=1}^{|\mathcal{J}_g|} \lambda_j \chi_{1,j}^2, \quad (20)$$

555 where $|\mathcal{J}_g|$ denotes the cardinality of the set of SNPs \mathcal{J}_g ; $\chi_{1,j}^2$ are standard chi-square random variables
 556 with one degree of freedom; and $(\lambda_1, \dots, \lambda_{|\mathcal{J}_g|})$ are the eigenvalues of the matrix [83, 84]

$$557 \quad \mathbb{V}[\tilde{\boldsymbol{\beta}}_g]^{1/2} \mathbf{A} \mathbb{V}[\tilde{\boldsymbol{\beta}}_g]^{1/2} = \sigma_\varepsilon^2 \boldsymbol{\Sigma}_g^{1/2} \mathbf{A} \boldsymbol{\Sigma}_g^{1/2}.$$

558 Again, in the current study, $\sigma_\varepsilon^2 = \hat{\sigma}_2^2$ from the estimates in Eq. (15), and $\boldsymbol{\Sigma}_g$ denotes a subset of the LD
 559 matrix only containing SNPs annotated in the g -th SNP-set. Again, when $\mathbf{A} = \mathbf{I}$, the eigenvalues are
 560 based on a scaled version of the local gene-specific LD matrix. Several approximate and exact methods
 561 have been suggested to obtain P -values under a mixture of chi-square distributions. In this study, we
 562 use Imhof's method [26] where we empirically compute an estimate of the weighted sum in Eq. (20) and

563 compare this distribution to the observed test statistic in Eq. (19) (see Software Details). It is important
 564 to note here that the gene-level null hypothesis is the same for gene- ε and other similar competing
 565 enrichment methods [9, 12, 20, 28, 58]; the defining characteristic that sets gene- ε apart is that it assumes
 566 a different null distribution for effects on the SNP-level.

567 **Estimating Gene Specific Contributions to the PVE.** In the main text, we highlight some of the
 568 additional features of the gene- ε gene-level association test statistic. First, the expected enrichment for
 569 trait-associated mutations in a given gene is equal to the heritability explained by the SNPs contained in
 570 said gene. Formally, consider the expansion of Eq. (19) derived from the expectation of quadratic forms,

$$571 \quad \mathbb{E}[\tilde{Q}_g] = \sum_{j=1}^{|\mathcal{J}_g|} \sum_{j'=1}^{|\mathcal{J}_g|} a_{jj'} \mathbb{E}[\tilde{\beta}_j \tilde{\beta}_{j'}] = h_g^2, \quad (21)$$

572 where denotes the heritability contributed by gene g . When $\mathbf{A} = \mathbf{I}$ (as in the current study), the gene-
 573 ε hypothesis test for identifying enriched genes is based on the individual SNP contributions to the
 574 narrow-sense heritability (i.e., the sum of the expectation of squared SNP effects; see also [34])

$$575 \quad \mathbb{E}[\tilde{Q}_g] = \sum_{j=1}^{|\mathcal{J}_g|} \mathbb{E}[\tilde{\beta}_j^2] = h_g^2. \quad (22)$$

576 Alternatively, one could choose to re-weight these contributions by specifying \mathbf{A} otherwise [12, 20, 83, 85,
 577 86]. For example, if SNP j has a small effect size but is known to be functionally associated with the
 578 trait of interest, then increasing \mathbf{A}_{jj} will reflect this knowledge. Specific weight functions have also been
 579 suggested for dealing with rarer variants [9, 28, 58].

580 Simulation Studies

581 We used a simulation scheme to generate SNP-level summary statistics for GWA studies. First, we ran-
 582 domly select a set of enriched genes and assume that complex traits (under various genetic architectures)
 583 are generated via a linear model

$$584 \quad \mathbf{y} = \mathbf{W}\mathbf{b} + \sum_{c \in \mathcal{C}} \mathbf{x}_c \beta_c + \mathbf{e}, \quad \mathbf{e} \sim \mathcal{N}(\mathbf{0}, \tau^2 \mathbf{I}), \quad (23)$$

585 where \mathbf{y} is an N -dimensional vector containing all the phenotypes; \mathcal{C} represents the set of causal SNPs
 586 contained within the associated genes; \mathbf{x}_c is the genotype for the c -th causal SNP encoded as 0, 1, or
 587 2 copies of a reference allele; β_c is the additive effect size for the c -th SNP; \mathbf{W} is an $N \times M$ matrix of
 588 covariates representing additional population structure (e.g., the top ten principal components from the
 589 genotype matrix) with corresponding fixed effects \mathbf{b} ; and \mathbf{e} is an N -dimensional vector of environmental
 590 noise. The phenotypic variance is assumed $\mathbb{V}[\mathbf{y}] = 1$. The effect sizes of SNPs in enriched genes are
 591 randomly drawn from standard normal distributions and then rescaled so they explain a fixed proportion
 592 of the narrow-sense heritability $\mathbb{V}[\sum \mathbf{x}_c \beta_c] = h^2$. The covariate coefficients are also drawn from standard
 593 normal distributions and then rescaled such that $\mathbb{V}[\mathbf{W}\mathbf{b}] + \mathbb{V}[\mathbf{e}] = (1 - h^2)$. GWA summary statistics
 594 are then computed by fitting a single-SNP univariate linear model via ordinary least squares (OLS):
 595 $\hat{\beta}_j = (\mathbf{x}_j^T \mathbf{x}_j)^{-1} \mathbf{x}_j^T \mathbf{y}$ for every SNP in the data $j = 1, \dots, J$. These effect size estimates, along with an LD
 596 matrix Σ computed directly from the full $N \times J$ genotype matrix \mathbf{X} , are given to gene- ε . We also retain
 597 standard errors and P -values for implementation of the competing methods (VEGAS, PEGASUS, RSS,
 598 SKAT, and MAGMA). Given different model parameters, we simulate data mirroring a wide range of
 599 genetic architectures (Supporting Information).

600 Software Details

601 Source code implementing gene- ε and tutorials are freely available at [https://github.com/ramachandran-lab/](https://github.com/ramachandran-lab/genee)
602 **genee** and was written in R (version 3.3.3). Within this software, regularization of the OLS SNP-level
603 effect sizes is done using the package **glmnet** (version 2.0-16) [87]. For large datasets, such as the UK
604 Biobank, the software also offers regularization using the **biglasso** (version 1.3-6) [88] to help with
605 memory and scalability requirements. Note that selection of the free parameter t is done the same way
606 using both the **glmnet** and **biglasso** packages. Both packages also take in an $\alpha \in [0, 1]$ to specify fit-
607 ting the Ridge, Elastic Net or Lasso regularization to the OLS SNP-level effect sizes. The fitting of a
608 K -mixture of Gaussian distributions for the estimation of the SNP-level null threshold σ_ε^2 is done using
609 the package **mclust** (version 5.4.3) [81]. Lastly, the package **CompQuadForm** (version 1.4.3) was used to
610 compute gene- ε gene-level P -values with Imhof's method [26, 89]. Comparisons in this work were made
611 using software for MAGMA (version 1.07b; <https://ctg.cncr.nl/software/magma>), PEGASUS (ver-
612 sion 1.3.0; <https://github.com/ramachandran-lab/PEGASUS>), RSS (version 1.0.0; <https://github.com/stephenslab/rss>), SKAT (version 1.3.2.1; <https://www.hsph.harvard.edu/skat>), VEGAS (ver-
613 sion 2.0.0; <https://vegas2.qimrberghofer.edu.au>) which are also publicly available. See all other
614 relevant URLs below.
615

616 URLs

617 gene- ε software, <https://github.com/ramachandran-lab/genee>; UK Biobank, [https://www.ukbiobank.](https://www.ukbiobank.ac.uk)
618 [ac.uk](https://www.ukbiobank.ac.uk); Database of Genotypes and Phenotypes (dbGaP), <https://www.ncbi.nlm.nih.gov/gap>; NHGRI-
619 EBI GWAS Catalog, <https://www.ebi.ac.uk/gwas/>; UCSC Genome Browser, [https://genome.ucsc.](https://genome.ucsc.edu/index.html)
620 [edu/index.html](https://genome.ucsc.edu/index.html); Enrichr software, <http://amp.pharm.mssm.edu/Enrichr/>; SNP-set (Sequence) Ker-
621 nel Association Test (SKAT) software, <https://www.hsph.harvard.edu/skat>; Multi-marker Analysis
622 of GenoMic Annotation (MAGMA) software, <https://ctg.cncr.nl/software/magma>; Precise, Efficient
623 Gene Association Score Using SNPs (PEGASUS) software, [https://github.com/ramachandran-lab/](https://github.com/ramachandran-lab/PEGASUS)
624 [PEGASUS](https://github.com/ramachandran-lab/PEGASUS); Regression with Summary Statistics (RSS) enrichment software, [https://github.com/stephenslab/](https://github.com/stephenslab/rss)
625 [rss](https://github.com/stephenslab/rss); Versatile Gene-based Association Study (VEGAS) version 2, [https://vegas2.qimrberghofer.](https://vegas2.qimrberghofer.edu.au)
626 [edu.au](https://vegas2.qimrberghofer.edu.au).

627 **Figures and Tables**

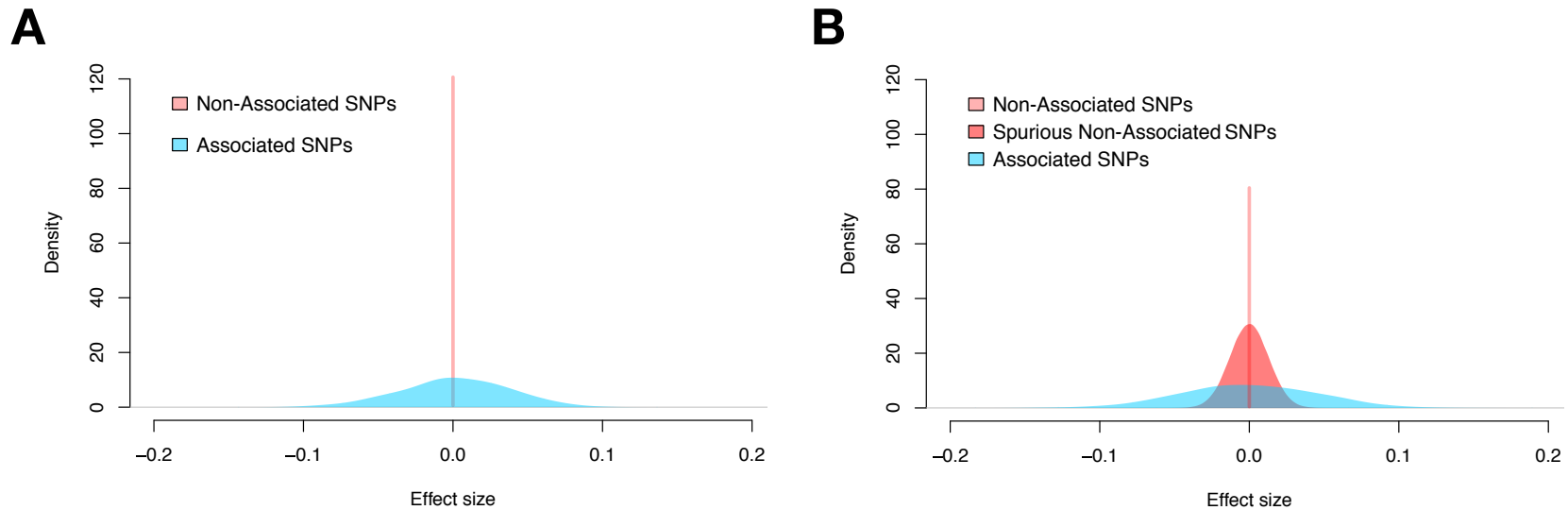


Figure 1. Illustration of null hypothesis assumptions for the distribution of GWA SNP-level effect sizes according to different views on underlying genetic architectures. The effect sizes of “non-associated” (pink), “spurious non-associated” (red), and “associated” (blue) SNPs were drawn from normal distributions with successively larger variances. **(A)** The traditional GWA model of complex traits simply assumes SNPs are associated or non-associated. Under the corresponding null hypothesis, associated SNPs are likely to emit nonzero effect sizes while non-associated SNPs will have effect sizes of zero. When there are many causal variants, we refer to the traits as polygenic. **(B)** Under our reformulated GWA model, there are three categories: associated SNPs, non-associated SNPs that emit spurious nonzero effect sizes, and non-associated SNPs with effect sizes of zero. We propose a multi-component framework (see also [18]), in which null SNPs can emit different levels of statistical signals based on (*i*) different degrees of connectedness (e.g., through linkage disequilibrium), or (*ii*) its regulated gene interacts with an enriched gene. While truly associated SNPs are still more likely to emit large effect sizes than SNPs in the other categories, null SNPs can have intermediate effect sizes. Here, our goal is to treat spurious SNPs with small-to-intermediate nonzero effects as being non-associated with the trait of interest.

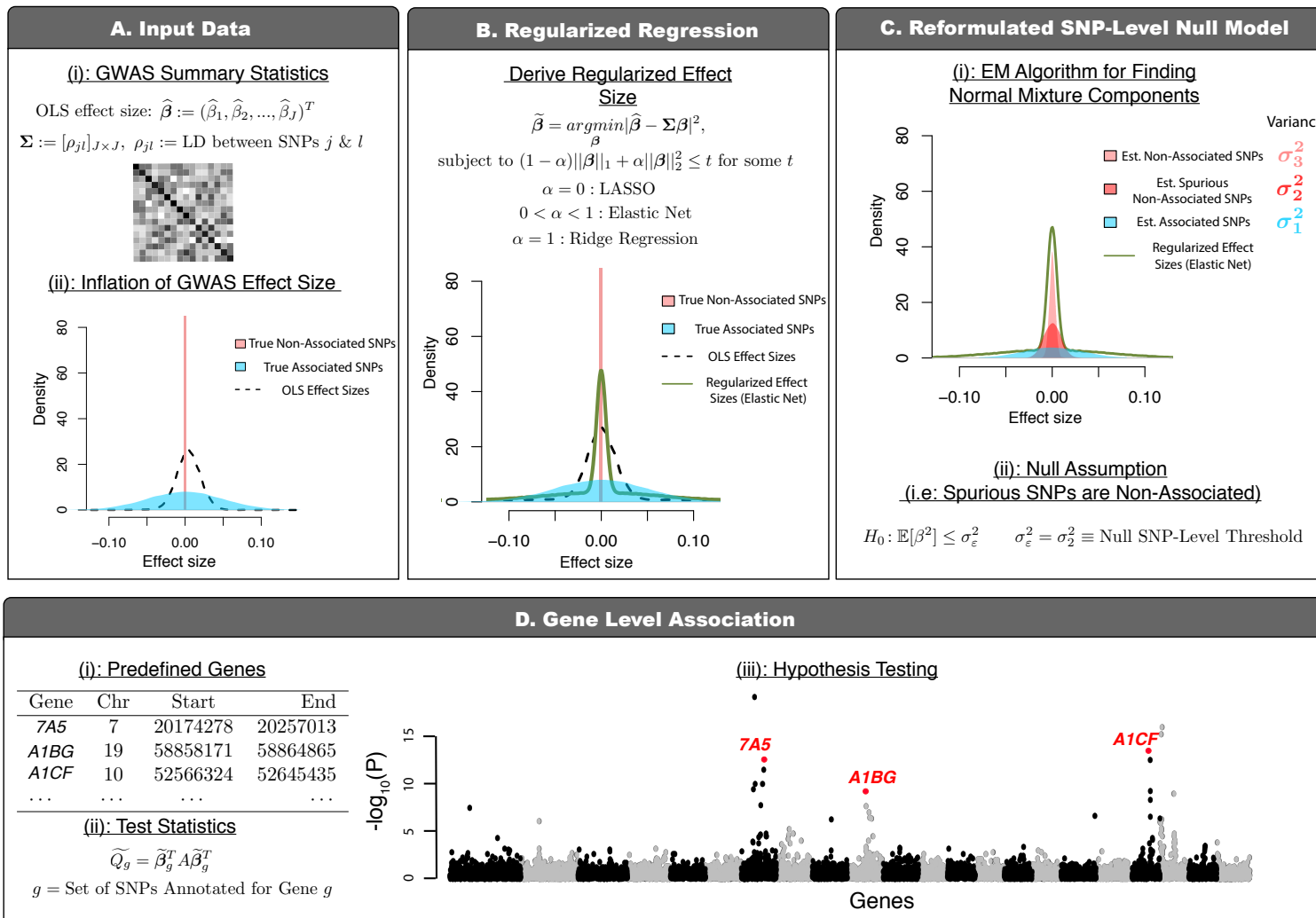


Figure 2. Schematic overview of gene- ε : our new gene-level association approach accounting for spurious nonzero SNP-level effects. (A) gene- ε takes SNP-level GWA marginal effect sizes (OLS estimates $\hat{\beta}$) and a linkage disequilibrium (LD) matrix (Σ) as input. It is well-known that OLS effect size estimates are inflated due to LD (i.e., correlation structures) among genome-wide genotypes. (B) gene- ε first uses its inputs to derive regularized effect size estimates ($\tilde{\beta}$) through shrinkage methods (LASSO, Elastic Net and Ridge Regression; we explore performance of each solution under a variety of simulated trait architectures in Supporting Information). (C) A unique feature of gene- ε is that it treats SNPs with spurious nonzero effects as non-associated. gene- ε assumes a reformulated null distribution of SNP-level effects $\tilde{\beta}_j \sim \mathcal{N}(0, \sigma_\varepsilon^2)$, where σ_ε^2 is the SNP-level null threshold and represents the maximum proportion of phenotypic variance explained (PVE) by a spurious or non-associated SNP. This leads to the reformulated SNP-level null hypothesis $H_0 : \mathbb{E}[\beta_j^2] \leq \sigma_\varepsilon^2$. To infer an appropriate σ_ε^2 , gene- ε fits a K -mixture of normal distributions over the regularized effect sizes with successively smaller variances ($\sigma_1^2 > \dots > \sigma_K^2$; with $\sigma_K^2 = 0$). In this study (without loss of generality), we assume that associated SNPs will appear in the first set, while spurious and non-associated SNPs appear in the latter sets. By definition, the SNP-level null threshold is then $\sigma_\varepsilon^2 = \sigma_2^2$. (D) Lastly, gene- ε computes gene-level association test statistics \tilde{Q}_g using quadratic forms and corresponding P -values using Imhof's method. This assumes the common gene-level null $H_0 : Q_g = 0$, where the null distribution of Q_g is dependent upon the SNP-level null threshold σ_ε^2 . For more details, see Materials and Methods.

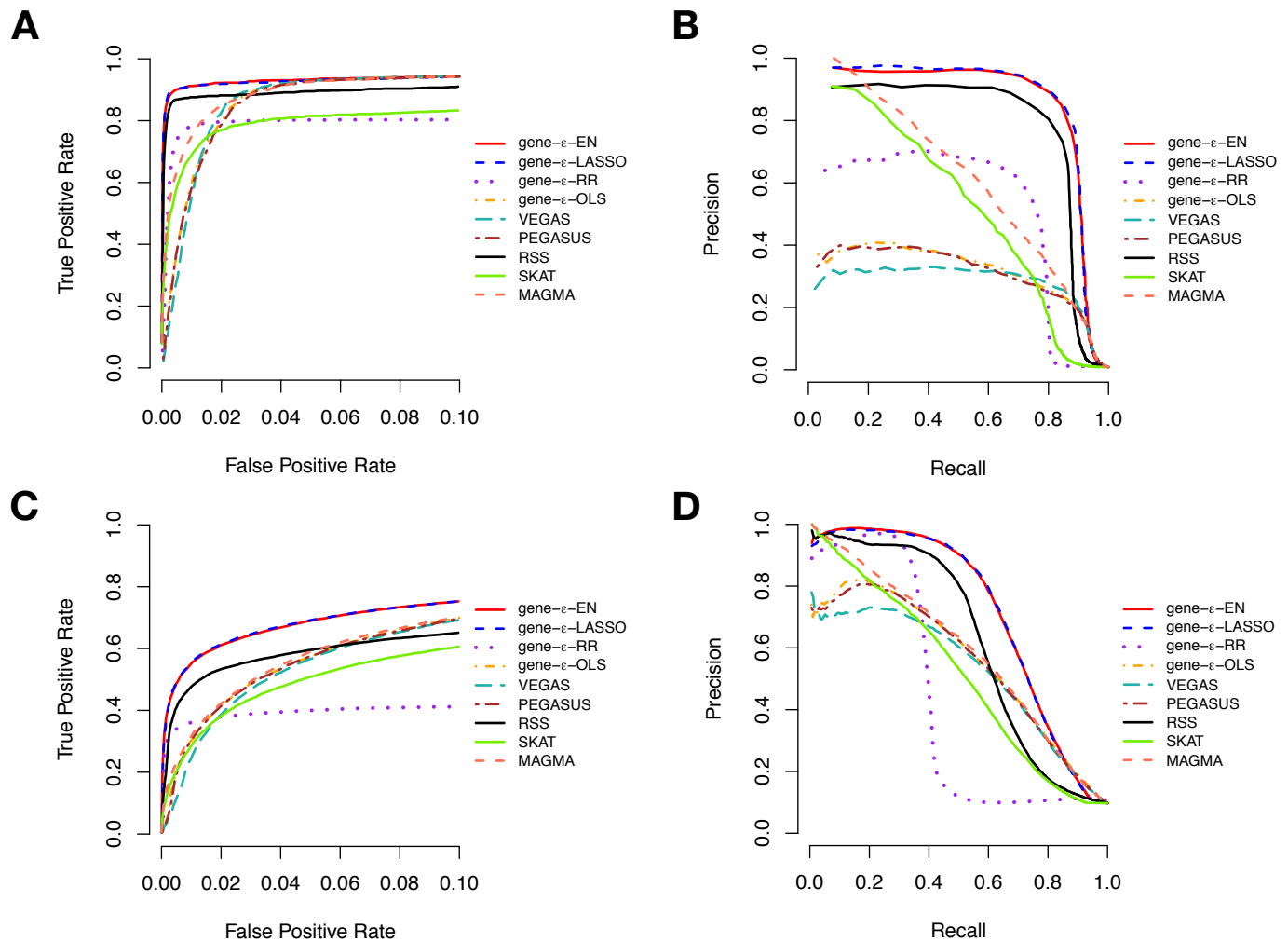


Figure 3. Receiver operating characteristic (ROC) and precision-recall curves comparing the performance of gene- ϵ and competing approaches in simulations ($N = 10,000$; $h^2 = 0.6$). We simulate complex traits under different genetic architectures and GWA study scenarios, varying the following parameters: narrow sense heritability, proportion of associated genes, and sample size (Supporting Information). Here, the sample size $N = 10,000$ and the narrow-sense heritability $h^2 = 0.6$. We compute standard GWA SNP-level effect sizes (estimated using ordinary least squares). Results for gene- ϵ are shown with LASSO (blue), Elastic Net (EN; red), and Ridge Regression (RR; purple) regularizations. We also show the results of gene- ϵ without regularization to illustrate the importance of this step (labeled OLS; orange). We further compare gene- ϵ with five existing methods: PEGASUS (brown) [12], VEGAS (teal) [7], the Bayesian approach RSS (black) [14], SKAT (green) [20], and MAGMA (peach) [10]. **(A, C)** ROC curves show power versus false positive rate for each approach of sparse (1% associated genes) and polygenic (10% associated genes) architectures, respectively. Note that the upper limit of the x-axis has been truncated at 0.1. **(B, D)** Precision-Recall curves for each method applied to the simulations. Note that, in the sparse case (1% associated genes), the top ranked genes are always true positives, and therefore the minimal recall is not 0. All results are based on 100 replicates.

# Total Genes	# SNPs per Gene	<i>Average Time (sec)</i>					
		gene- ϵ	PEGASUS	VEGAS	RSS	MAGMA	SKAT
250	5	2.18	2.99	39.18	3.33	<0.10	1.17
	10	4.34	1.55	57.22	13.81	<0.10	1.90
	20	12.94	1.22	85.54	55.49	<0.10	3.63
500	5	8.62	6.10	77.35	14.70	<0.10	2.25
	10	16.00	3.37	106.05	56.38	<0.10	4.08
	20	37.88	2.52	194.21	248.90	<0.10	7.07
1000	5	25.89	11.81	152.12	60.11	0.28	4.87
	10	40.69	6.33	200.78	250.51	0.58	8.59
	20	136.96	6.87	284.97	9410.37	1.19	14.21

Table 1. Computational time for running gene- ϵ and other gene-level association approaches, as a function of the total number genes analyzed and the number of SNPs within each gene. Methods compared include: gene- ϵ , PEGASUS [12], VEGAS [7], RSS [14], MAGMA [10], and SKAT [20]. Here, we simulated 10 datasets for each pair of parameter values (number of genes analyzed, and number of SNPs within each gene). Each table entry represents the average computation time (in seconds) it takes each approach to analyze a dataset of the size indicated. Run times were measured on a MacBook Pro (Processor: 3.1-gigahertz (GHz) Intel Core i5, Memory: 8GB 2133-megahertz (MHz) LPDDR3). Only a single core on the machine was used. PEGASUS, SKAT, and MAGMA are score-based methods and, thus, are expected to take the least amount of time to run. Both gene- ϵ and RSS are regression-based methods, but gene- ϵ is scalable in both the number of genes and the number of SNPs per gene. The increased computational burden of RSS results from its need to do Bayesian posterior inference; however, gene- ϵ is able to scale because it leverages regularization and point estimation for hypothesis testing.

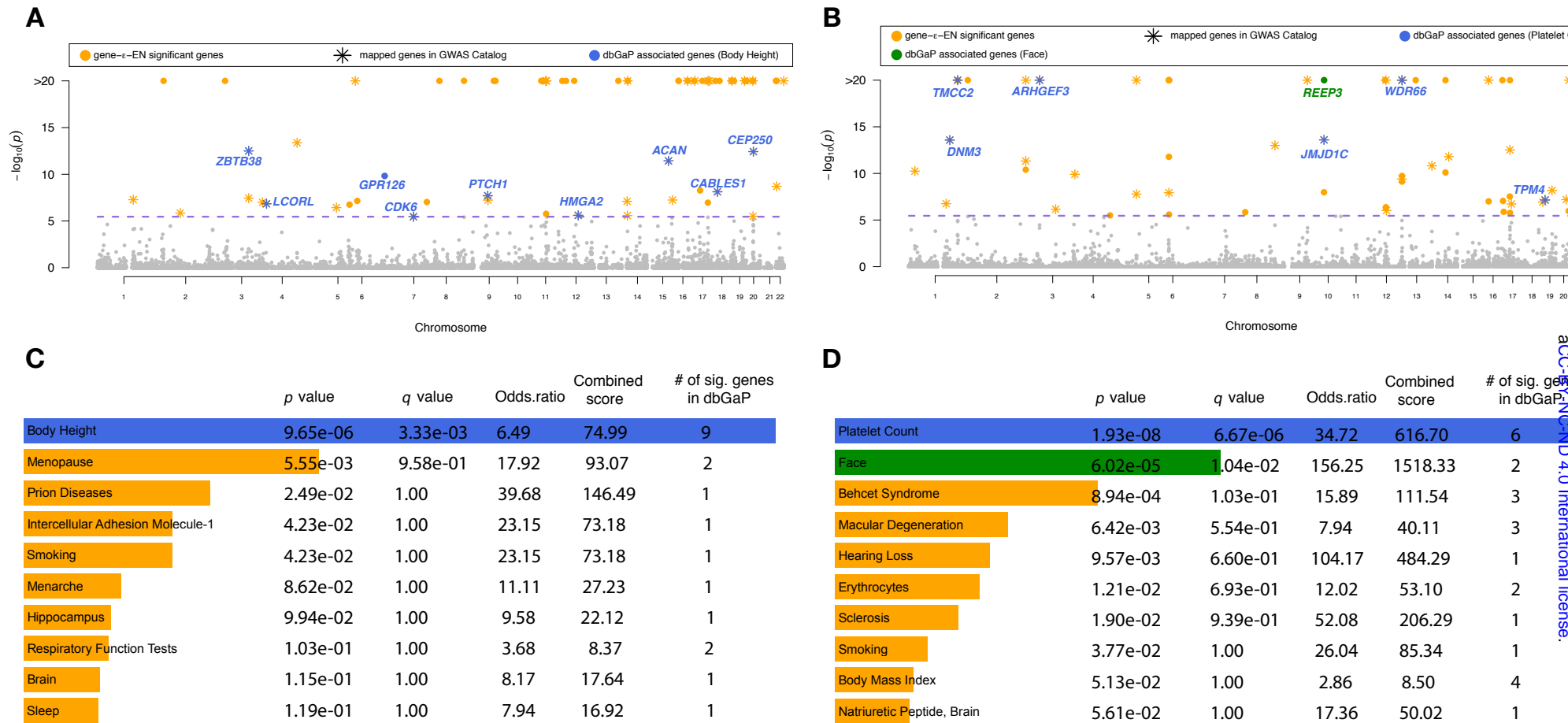


Figure 4. Gene-level association results from applying gene- ϵ to body height (panels A and C) and mean platelet volume (MPV; panels B and D), assayed in European-ancestry individuals in the UK Biobank. Body height has been estimated to have a narrow-sense heritability h^2 in the range of 0.45 to 0.80 [6, 31–39]; while, MPV has been estimated to have h^2 between 0.50 and 0.70 [33, 34, 90]. Manhattan plots of gene- ϵ gene-level association P -values using Elastic Net regularized effect sizes for (A) body height and (B) MPV. The purple dashed line indicates a log-transformed Bonferroni-corrected significance threshold ($P = 3.49 \times 10^{-6}$ correcting for 14,322 autosomal genes analyzed). We color code all significant genes identified by gene- ϵ in orange, and annotate genes overlapping with the database of Genotypes and Phenotypes (dbGaP). In (C) and (D), we conduct gene set enrichment analysis using Enrichr [46, 91] to identify dbGaP categories enriched for significant gene-level associations reported by gene- ϵ . We highlight categories with Q -values (i.e., false discovery rates) less than 0.05 and annotate corresponding genes in the Manhattan plots in (A) and (B), respectively. For height, the only significant dbGAP category is “Body Height”, with nine of the genes identified by gene- ϵ appearing in this category. For MPV, the two significant dbGAP categories are “Platelet Count” and “Face” — the first of which is directly connected to trait [57, 92, 93].

Trait	Gene	Chr	gene- ϵ P -Value	Rank	h_g^2	Post. Prob.	Biological Relevance to Trait	Ref(s)
Height	<i>EZH2</i>	7	9.34×10^{-8}	61	7.23×10^{-3}	1.000	Associated with diseases Adamantinoma of Long Bone and Weaver Syndrome (characterized by rapid growth).	[94]
Height	<i>C17orf42</i>	17	5.38×10^{-9}	52	4.54×10^{-3}	1.000	Known as the transcription elongation factor of mitochondria (TEFM) which regulates transcription and can affect body height.	[95]
Height	<i>KISS1R</i>	19	1×10^{-20}	1*	5.27×10^{-4}	0.970	Associated with disorders of puberty and final height.	[96]
BMI	<i>ZC3H4</i>	19	1.62×10^{-14}	20	7.84×10^{-3}	1.000	BMI-inducer known to be associated with adiposity and obesity.	[97–100]
BMI	<i>PTOV1</i>	19	1×10^{-20}	1*	2.26×10^{-3}	0.990	Found to be overexpressed in prostate adenocarcinomas which can be induced by obesity.	[101]
BMI	<i>FBXO45</i> ♣	3	6.52×10^{-7}	23	1.82×10^{-3}	0.029	Reported to be involved in children syndromic obesity.	[102]
MCV	<i>SLC24A1</i>	15	1.74×10^{-7}	50	4.66×10^{-3}	0.140	Encoded protein is involved in glucose transportation pathway and MCV is reported to be associated with glucose level.	[101]
MCV	<i>PDX1</i> ♣	13	1×10^{-20}	1*	2.31×10^{-4}	0.019	Associated with Glycated hemoglobin which is affected by MCV	[103]
MCV	<i>RHOD</i>	11	1×10^{-20}	1*	3.35×10^{-4}	0.002	Associated with Wiskott-Aldrich Syndrome which is characterized by abnormal immune system function (immune deficiency) and a reduced ability to form blood clots.	[101, 104]
MPV	<i>C1orf150</i>	1	1×10^{-20}	1*	3.44×10^{-2}	1.000	Known as <i>GCSAML</i> which is involved with germinal center signaling and differentiation of mature B cells that mutually activate platelets.	[47–49]
MPV	<i>KIAA0922</i>	4	3.20×10^{-6}	64	7.17×10^{-3}	1.000	Known as <i>TMEM131L</i> which is associated with canonical Wnt signaling and can effect platelet formation.	[105, 106]
MPV	<i>TPT1</i> ♣	13	1×10^{-20}	1*	3.25×10^{-4}	0.051	mRNA expression is identified in platelets.	[101]
PLC	<i>C1orf150</i>	1	1×10^{-20}	1*	2.51×10^{-2}	1.000	Known as <i>GCSAML</i> which is involved with germinal center signaling and differentiation of mature B cells that mutually activate platelets.	[47–49]
PLC	<i>PSMD2</i>	3	1.42×10^{-9}	29	7.40×10^{-3}	1.000	Also known as the 26S proteasome which is found to be important for platelet production.	[101]
PLC	<i>APOB48R</i>	16	1×10^{-20}	1*	1.36×10^{-3}	0.003	Involved in Lipoprotein metabolism pathway which can affect platelet.	[101]
WHR	<i>TFAP2B</i>	6	3.92×10^{-7}	21	3.60×10^{-3}	1.000	Dietary protein associated with weight maintenance.	[99, 107]
WHR	<i>WDR68</i>	17	1.05×10^{-7}	20	1.10×10^{-3}	0.990	Also known as <i>DCAF7</i> which has been shown to bind Huntingtin-associated protein 1 (HAP1) and affect weight.	[108]
WHR	<i>MLL</i>	11	8.14×10^{-8}	19	2.43×10^{-3}	0.940	Orthologous gene in mice that affects skeleton, body size, and growth.	[99, 109–111]

Table 2. Top three newly identified candidate genes reported by gene- ϵ for the six quantitative traits studied in the UK Biobank (using imputed genotypes with gene boundaries defined by the NCBI’s RefSeq database in the UCSC Genome Browser [27]). We call these novel candidate genes because they are not listed as being associated with the trait of interest in either the GWAS catalog or dbGaP, and they have top posterior enrichment probabilities with the trait using RSS analysis. Each gene is annotated with past functional studies that link them to the trait of interest. We also report each gene’s overall trait-specific significance rank (out of 14,322 autosomal genes analyzed for each trait), as well as their heritability estimates from gene- ϵ using Elastic Net to regularize GWA SNP-level effect size estimates. The traits are: height; body mass index (BMI); mean corpuscular volume (MCV); mean platelet volume (MPV); platelet count (PLC); and waist-hip ratio (WHR). ♣: Enriched genes whose top SNP is not marginally significant according to a genome-wide Bonferroni-corrected threshold ($P = 4.67 \times 10^{-8}$ correcting for 1,070,306 SNPs analyzed; see highlighted rows in Supplementary Tables S19-S24 for complete list). *: Multiple genes were tied for this ranking.

References

628

629

630

631

632

633

634

635

636

637

638

639

640

641

642

643

644

645

646

647

648

649

650

651

652

653

654

655

656

657

658

659

660

661

662

663

664

665

666

667

1. Visscher PM, Hill WG, Wray NR. Heritability in the genomics era—concepts and misconceptions. *Nat Rev Genet.* 2008;9(4):255–266.
2. Manolio TA, Collins FS, Cox NJ, Goldstein DB, Hindorff LA, Hunter DJ, et al. Finding the missing heritability of complex diseases. *Nature.* 2009;461(7265):747–753. Available from: <https://www.ncbi.nlm.nih.gov/pubmed/19812666>.
3. Visscher PM, Brown MA, McCarthy MI, Yang J. Five Years of GWAS Discovery. *Am J Hum Genet.* 2012;90(1):7–24. Available from: <http://www.sciencedirect.com/science/article/pii/S0002929711005337>.
4. Boyle EA, Li YI, Pritchard JK. An expanded view of complex traits: from polygenic to omnigenic. *Cell.* 2017;169(7):1177–1186.
5. Wray NR, Wijmenga C, Sullivan PF, Yang J, Visscher PM. Common disease is more complex than implied by the core gene omnigenic model. *Cell.* 2018;173(7):1573–1580. Available from: <https://doi.org/10.1016/j.cell.2018.05.051>.
6. Yang J, Benyamin B, McEvoy BP, Gordon S, Henders AK, Nyholt DR, et al. Common SNPs explain a large proportion of the heritability for human height. *Nat Genet.* 2010;42(7):565–569.
7. Liu JZ, Mcrae AF, Nyholt DR, Medland SE, Wray NR, Brown KM, et al. A versatile gene-based test for genome-wide association studies. *Am J Hum Genet.* 2010;87(1):139–145.
8. Carbonetto P, Stephens M. Integrated enrichment analysis of variants and pathways in genome-wide association studies indicates central role for IL-2 signaling genes in type 1 diabetes, and cytokine signaling genes in Crohn’s disease. *PLoS Genet.* 2013;9(10):e1003770–. Available from: <https://doi.org/10.1371/journal.pgen.1003770>.
9. Ionita-Laza I, Lee S, Makarov V, Buxbaum JD, Lin X. Sequence kernel association tests for the combined effect of rare and common variants. *Am J Hum Genet.* 2013;92(6):841–853. Available from: <http://www.sciencedirect.com/science/article/pii/S0002929713001766>.
10. de Leeuw CA, Mooij JM, Heskes T, Posthuma D. MAGMA: generalized gene-set analysis of GWAS data. *PLOS Comput Biol.* 2015;11(4):e1004219–. Available from: <https://doi.org/10.1371/journal.pcbi.1004219>.
11. Lamparter D, Marbach D, Rueedi R, Kutalik Z, Bergmann S. Fast and rigorous computation of gene and pathway scores from SNP-based summary statistics. *PLOS Comput Biol.* 2016;12(1):e1004714–. Available from: <https://doi.org/10.1371/journal.pcbi.1004714>.
12. Nakka P, Raphael BJ, Ramachandran S. Gene and network analysis of common variants reveals novel associations in multiple complex diseases. *Genetics.* 2016;204(2):783–798. Available from: <http://www.genetics.org/content/204/2/783.abstract>.
13. Wang M, Huang J, Liu Y, Ma L, Potash JB, Han S. COMBAT: a combined association test for genes using summary statistics. *Genetics.* 2017;207(3):883–891.
14. Zhu X, Stephens M. Large-scale genome-wide enrichment analyses identify new trait-associated genes and pathways across 31 human phenotypes. *Nat Comm.* 2018;9(1):4361.
15. Zhou X, Carbonetto P, Stephens M. Polygenic modeling with Bayesian sparse linear mixed models. *PLoS Genet.* 2013;9(2):e1003264.

- 668 16. Yang J, Zaitlen NA, Goddard ME, Visscher PM, Price AL. Advantages and pitfalls in the
669 application of mixed-model association methods. *Nat Genet.* 2014;46(2):100–106.
- 670 17. Bulik-Sullivan BK, Loh PR, Finucane HK, Ripke S, Yang J, of the Psychiatric Genomics Consor-
671 tium SWG, et al. LD Score regression distinguishes confounding from polygenicity in genome-wide
672 association studies. *Nat Genet.* 2015;47:291–295. Available from: [http://dx.doi.org/10.1038/
673 ng.3211](http://dx.doi.org/10.1038/ng.3211).
- 674 18. Zhang Y, Qi G, Park JH, Chatterjee N. Estimation of complex effect-size distributions using
675 summary-level statistics from genome-wide association studies across 32 complex traits. *Nat*
676 *Genet.* 2018;50(9):1318–1326.
- 677 19. Holland D, Wang Y, Thompson WK, Schork A, Chen CH, Lo MT, et al. Estimating Effect Sizes
678 and Expected Replication Probabilities from GWAS Summary Statistics. *Front Genet.* 2016;7:15.
679 Available from: <https://www.frontiersin.org/article/10.3389/fgene.2016.00015>.
- 680 20. Wu MC, Kraft P, Epstein MP, Taylor DM, Chanock SJ, Hunter DJ, et al. Powerful SNP-set
681 analysis for case-control genome-wide association studies. *Am J Hum Genet.* 2010;86(6):929–942.
- 682 21. Bycroft C, Freeman C, Petkova D, Band G, Elliott LT, Sharp K, et al. The UK Biobank resource
683 with deep phenotyping and genomic data. *Nature.* 2018;562(7726):203–209. Available from:
684 <https://doi.org/10.1038/s41586-018-0579-z>.
- 685 22. Stephens M. False discovery rates: a new deal. *Biostatistics.* 2017;18(2):275–294. Available from:
686 <http://dx.doi.org/10.1093/biostatistics/kxw041>.
- 687 23. Tibshirani R. Regression shrinkage and selection via the lasso. *J R Stat Soc Series B Stat*
688 *Methodol.* 1996;58(1):267–288.
- 689 24. Zou H, Hastie T. Regularization and variable selection via the elastic net. *J R Stat Soc Series B*
690 *Stat Methodol.* 2005;67(2):301–320.
- 691 25. Hoerl AE, Kennard RW. Ridge regression: Biased estimation for nonorthogonal problems. *Tech-*
692 *nometrics.* 1970;12(1):55–67.
- 693 26. Imhof JP. Computing the distribution of quadratic forms in normal variables. *Biometrika.*
694 1961;48(3/4):419–426. Available from: <http://www.jstor.org/stable/2332763>.
- 695 27. Pruitt KD, Tatusova T, Maglott DR. NCBI Reference Sequence (RefSeq): a curated non-
696 redundant sequence database of genomes, transcripts and proteins. *Nucleic Acids Res.*
697 2005;33(Database issue):D501–4.
- 698 28. Lee S, Emond MJ, Bamshad MJ, Barnes KC, Rieder MJ, Nickerson DA, et al. Optimal unified
699 approach for rare-variant association testing with application to small-sample case-control whole-
700 exome sequencing studies. *Am J Hum Genet.* 2012;91(2):224–237. Available from: [http://www.
701 sciencedirect.com/science/article/pii/S0002929712003163](http://www.sciencedirect.com/science/article/pii/S0002929712003163).
- 702 29. Zhu X, Stephens M. Bayesian large-scale multiple regression with summary statistics from
703 genome-wide association studies. *Ann Appl Stat.* 2017;11(3):1561–1592. Available from: [https:
704 //projecteuclid.org:443/euclid.aoas/1507168840](https://projecteuclid.org:443/euclid.aoas/1507168840).
- 705 30. Barbieri MM, Berger JO. Optimal predictive model selection. *Ann Statist.* 2004;32(3):870–897.
706 Available from: <http://projecteuclid.org/euclid.aos/1085408489>.

- 707 31. Zaitlen N, Kraft P, Patterson N, Pasaniuc B, Bhatia G, Pollack S, et al. Using extended genealogy
708 to estimate components of heritability for 23 quantitative and dichotomous traits. *PLoS Genet.*
709 2013;9(5):e1003520-. Available from: <https://doi.org/10.1371/journal.pgen.1003520>.
- 710 32. Wood AR, Esko T, Yang J, Vedantam S, Pers TH, Gustafsson S, et al. Defining the role of
711 common variation in the genomic and biological architecture of adult human height. *Nat Genet.*
712 2014;46(11):1173–1186.
- 713 33. Heckerman D, Gurdasani D, Kadie C, Pomilla C, Carstensen T, Martin H, et al. Linear mixed
714 model for heritability estimation that explicitly addresses environmental variation. *Proc Natl*
715 *Acad Sci U S A.* 2016;113(27):7377–7382. Available from: [http://www.pnas.org/content/113/](http://www.pnas.org/content/113/27/7377.abstract)
716 [27/7377.abstract](http://www.pnas.org/content/113/27/7377.abstract).
- 717 34. Shi H, Kichaev G, Pasaniuc B. Contrasting the genetic architecture of 30 complex traits from
718 summary association data. *Am J Hum Genet.* 2016;99(1):139–153. Available from: [http://www.](http://www.sciencedirect.com/science/article/pii/S0002929716301483)
719 [sciencedirect.com/science/article/pii/S0002929716301483](http://www.sciencedirect.com/science/article/pii/S0002929716301483).
- 720 35. Xia C, Amador C, Huffman J, Trochet H, Campbell A, Porteous D, et al. Pedigree- and SNP-
721 associated genetics and recent environment are the major contributors to anthropometric and
722 cardiometabolic trait variation. *PLoS Genet.* 2016;12(2):e1005804-. Available from: [https:](https://doi.org/10.1371/journal.pgen.1005804)
723 [//doi.org/10.1371/journal.pgen.1005804](https://doi.org/10.1371/journal.pgen.1005804).
- 724 36. Ge T, Chen CY, Neale BM, Sabuncu MR, Smoller JW. Phenome-wide heritability analysis of the
725 UK Biobank. *PLoS Genet.* 2017;13(4):e1006711-. Available from: [https://doi.org/10.1371/](https://doi.org/10.1371/journal.pgen.1006711)
726 [journal.pgen.1006711](https://doi.org/10.1371/journal.pgen.1006711).
- 727 37. Speed D, Cai N, The UCLEB Consortium, Johnson MR, Nejentsev S, Balding DJ. Reevaluation
728 of SNP heritability in complex human traits. *Nat Genet.* 2017;49:986–992. Available from:
729 <https://doi.org/10.1038/ng.3865>.
- 730 38. Marouli E, Graff M, Medina-Gomez C, Lo KS, Wood AR, Kjaer TR, et al. Rare and low-frequency
731 coding variants alter human adult height. *Nature.* 2017;542(7640):186–190.
- 732 39. Wainschtein P, Jain DP, Yengo L, Zheng Z, TOPMed Anthropometry Working Group, Trans-
733 Omics for Precision Medicine Consortium, et al. Recovery of trait heritability from whole genome
734 sequence data. *bioRxiv.* 2019;p. 588020. Available from: [http://biorxiv.org/content/early/](http://biorxiv.org/content/early/2019/03/25/588020.abstract)
735 [2019/03/25/588020.abstract](http://biorxiv.org/content/early/2019/03/25/588020.abstract).
- 736 40. Goldstein DB. Common genetic variation and human traits. *N Engl J Med.* 2009;360(17):1696–
737 1698.
- 738 41. Lello L, Avery SG, Tellier L, Vazquez AI, de los Campos G, Hsu SDH. Accurate Genomic Predic-
739 tion of Human Height. *Genetics.* 2018;210(2):477–497. Available from: [http://www.genetics.](http://www.genetics.org/content/210/2/477.abstract)
740 [org/content/210/2/477.abstract](http://www.genetics.org/content/210/2/477.abstract).
- 741 42. Vattikuti S, Guo J, Chow CC. Heritability and genetic correlations explained by common SNPs
742 for metabolic syndrome traits. *PLoS Genet.* 2012;8(3):e1002637.
- 743 43. Yang J, Bakshi A, Zhu Z, Hemani G, Vinkhuyzen AA, Lee SH, et al. Genetic variance estimation
744 with imputed variants finds negligible missing heritability for human height and body mass index.
745 *Nat Genet.* 2015;47(10):1114.
- 746 44. Robinson MR, English G, Moser G, Lloyd-Jones LR, Triplett MA, Zhu Z, et al. Genotype-
747 covariate interaction effects and the heritability of adult body mass index. *Nat Genet.*
748 2017;49(8):1174.

- 749 45. Rothschild D, Weissbrod O, Barkan E, Kurilshikov A, Korem T, Zeevi D, et al. Environment dom-
750 inates over host genetics in shaping human gut microbiota. *Nature*. 2018;555:210–215. Available
751 from: <https://doi.org/10.1038/nature25973>.
- 752 46. Chen EY, Tan CM, Kou Y, Duan Q, Wang Z, Meirelles GV, et al. Enrichr: interactive and col-
753 laborative HTML5 gene list enrichment analysis tool. *BMC Bioinform*. 2013;14(1):128. Available
754 from: <https://doi.org/10.1186/1471-2105-14-128>.
- 755 47. Roadmap Epigenomics Consortium, Kundaje A, Meuleman W, Ernst J, Bilenky M, Yen A, et al.
756 Integrative analysis of 111 reference human epigenomes. *Nature*. 2015;518(7539):317–330. Avail-
757 able from: <https://www.ncbi.nlm.nih.gov/pubmed/25693563>.
- 758 48. Eicher JD, Chami N, Kacprowski T, Nomura A, Chen MH, Yanek LR, et al. Platelet-Related
759 Variants Identified by Exomechip Meta-analysis in 157,293 Individuals. *Am J Hum Genet*.
760 2016;99(1):40–55.
- 761 49. Iotchkova V, Huang J, Morris JA, Jain D, Barbieri C, Walter K, et al. Discovery and refinement
762 of genetic loci associated with cardiometabolic risk using dense imputation maps. *Nat Genet*.
763 2016;48(11):1303–1312. Available from: <https://www.ncbi.nlm.nih.gov/pubmed/27668658>.
- 764 50. Finberg KE, Heeney MM, Campagna DR, Aydinok Y, Pearson HA, Hartman KR, et al. Mutations
765 in *TMPRSS6* cause iron-refractory iron deficiency anemia (IRIDA). *Nat Genet*. 2008;40(5):569–
766 571. Available from: <https://www.ncbi.nlm.nih.gov/pubmed/18408718>.
- 767 51. Andrews NC. Genes determining blood cell traits. *Nat Genet*. 2009;41:1161–1162. Available from:
768 <https://doi.org/10.1038/ng1109-1161>.
- 769 52. Benyamin B, Ferreira MAR, Willemsen G, Gordon S, Middelberg RPS, McEvoy BP, et al. Com-
770 mon variants in *TMPRSS6* are associated with iron status and erythrocyte volume. *Nat Genet*.
771 2009;41(11):1173–1175.
- 772 53. Chambers JC, Zhang W, Li Y, Sehmi J, Wass MN, Zabaneh D, et al. Genome-wide asso-
773 ciation study identifies variants in *TMPRSS6* associated with hemoglobin levels. *Nat Genet*.
774 2009;41(11):1170–1172.
- 775 54. Soranzo N, Spector TD, Mangino M, Kühnel B, Rendon A, Teumer A, et al. A genome-wide
776 meta-analysis identifies 22 loci associated with eight hematological parameters in the HaemGen
777 consortium. *Nat Genet*. 2009;41(11):1182–1190. Available from: <https://www.ncbi.nlm.nih.gov/pubmed/19820697>.
- 778 55. Ganesh SK, Zakai NA, van Rooij FJA, Soranzo N, Smith AV, Nalls MA, et al. Multiple loci
779 influence erythrocyte phenotypes in the CHARGE Consortium. *Nat Genet*. 2009;41(11):1191–
780 1198.
- 781 56. Li J, Glessner JT, Zhang H, Hou C, Wei Z, Bradfield JP, et al. GWAS of blood cell traits identifies
782 novel associated loci and epistatic interactions in Caucasian and African-American children. *Hum*
783 *Mol Genet*. 2013;22(7):1457–1464. Available from: [https://www.ncbi.nlm.nih.gov/pubmed/](https://www.ncbi.nlm.nih.gov/pubmed/23263863)
784 [23263863](https://www.ncbi.nlm.nih.gov/pubmed/23263863).
- 785 57. Astle WJ, Elding H, Jiang T, Allen D, Ruklisa D, Mann AL, et al. The allelic landscape of
786 human blood cell trait variation and links to common complex disease. *Cell*. 2016;167(5):1415–
787 1429. Available from: <https://www.ncbi.nlm.nih.gov/pubmed/27863252>.
- 788 58. Wu MC, Lee S, Cai T, Li Y, Boehnke M, Lin X. Rare-variant association testing for sequencing
789 data with the sequence kernel association test. *Am J Hum Genet*. 2011;89(1):82–93.
790

- 791 59. Lee S, Abecasis GR, Boehnke M, Lin X. Rare-variant association analysis: study designs and sta-
792 tistical tests. *Am J Hum Genet.* 2014;95(1):5–23. Available from: <http://www.sciencedirect.com/science/article/pii/S0002929714002717>.
793
- 794 60. Zuk O, Schaffner SF, Samocha K, Do R, Hechter E, Kathiresan S, et al. Searching for missing her-
795 itability: designing rare variant association studies. *Proc Natl Acad Sci U S A.* 2014;111(4):E455–
796 E464. Available from: <http://www.pnas.org/content/111/4/E455.abstract>.
- 797 61. Gazal S, Loh PR, Finucane HK, Ganna A, Schoech A, Sunyaev S, et al. Functional architecture
798 of low-frequency variants highlights strength of negative selection across coding and non-coding
799 annotations. *Nat Genet.* 2018;50(11):1600–1607. Available from: <https://doi.org/10.1038/s41588-018-0231-8>.
800
- 801 62. Wojcik G, Graff M, Nishimura KK, Tao R, Haessler J, Gignoux CR, et al. The PAGE Study: how
802 genetic diversity improves our understanding of the architecture of complex traits. *bioRxiv.* 2018;p.
803 188094. Available from: <http://biorxiv.org/content/early/2018/10/17/188094.abstract>.
- 804 63. Martin AR, Kanai M, Kamatani Y, Okada Y, Neale BM, Daly MJ. Clinical use of current
805 polygenic risk scores may exacerbate health disparities. *Nat Genet.* 2019;51(4):584–591. Available
806 from: <https://doi.org/10.1038/s41588-019-0379-x>.
- 807 64. GTEx Consortium. Genetic effects on gene expression across human tissues. *Nature.*
808 2017;550:204–213. Available from: <https://doi.org/10.1038/nature24277>.
- 809 65. Wu Y, Zeng J, Zhang F, Zhu Z, Qi T, Zheng Z, et al. Integrative analysis of omics summary data
810 reveals putative mechanisms underlying complex traits. *Nat Comm.* 2018;9(1):918. Available
811 from: <https://doi.org/10.1038/s41467-018-03371-0>.
- 812 66. Xue A, Wu Y, Zhu Z, Zhang F, Kemper KE, Zheng Z, et al. Genome-wide association analyses
813 identify 143 risk variants and putative regulatory mechanisms for type 2 diabetes. *Nat Comm.*
814 2018;9(1):2941. Available from: <https://doi.org/10.1038/s41467-018-04951-w>.
- 815 67. Smemo S, Tena JJ, Kim KH, Gamazon ER, Sakabe NJ, Gomez-Marin C, et al. Obesity-
816 associated variants within FTO form long-range functional connections with IRX3. *Nature.*
817 2014;507(7492):371–375.
- 818 68. Claussnitzer M, Dankel SN, Kim KH, Quon G, Meuleman W, Haugen C, et al. FTO Obesity
819 Variant Circuitry and Adipocyte Browning in Humans. *N Engl J Med.* 2015;373(10):895–907.
820 Available from: <https://doi.org/10.1056/NEJMoa1502214>.
- 821 69. Lloyd-Jones LR, Zeng J, Sidorenko J, Yengo L, Moser G, Kemper KE, et al. Improved polygenic
822 prediction by Bayesian multiple regression on summary statistics. *Nat Comm.* 2019;10(1):5086.
823 Available from: <https://doi.org/10.1038/s41467-019-12653-0>.
- 824 70. Zeng P, Zhou X. Non-parametric genetic prediction of complex traits with latent Dirichlet pro-
825 cess regression models. *Nat Comm.* 2017;8:456. Available from: <https://doi.org/10.1038/s41467-017-00470-2>.
826
- 827 71. Lee SH, Wray NR, Goddard ME, Visscher PM. Estimating missing heritability for disease from
828 genome-wide association studies. *Am J Hum Genet.* 2011;88(3):294–305. Available from: <http://www.ncbi.nlm.nih.gov/pmc/articles/PMC3059431/>.
829
- 830 72. Golan D, Lander ES, Rosset S. Measuring missing heritability: inferring the contribution of
831 common variants. *Proc Natl Acad Sci U S A.* 2014;111(49):E5272–E5281. Available from: <http://www.pnas.org/content/111/49/E5272.abstract>.
832

- 833 73. Weissbrod O, Lippert C, Geiger D, Heckerman D. Accurate liability estimation improves power
834 in ascertained case-control studies. *Nat Meth.* 2015;12:332–334. Available from: <http://dx.doi.org/10.1038/nmeth.3285>.
835
- 836 74. Hormozdiari F, Kostem E, Kang EY, Pasaniuc B, Eskin E. Identifying causal variants at loci
837 with multiple signals of association. *Genetics.* 2014;198(2):497–508. Available from: <https://pubmed.ncbi.nlm.nih.gov/25104515>.
838
- 839 75. Hormozdiari F, van de Bunt M, Segrè AV, Li X, Joo JWJ, Bilow M, et al. Colocalization of GWAS
840 and eQTL Signals Detects Target Genes. *Am J Hum Genet.* 2016;99(6):1245–1260. Available from:
841 <https://doi.org/10.1016/j.ajhg.2016.10.003>.
- 842 76. Wold S, Ruhe A, Wold H, Dunn W III. The collinearity problem in linear regression. The partial
843 least squares (PLS) approach to generalized inverses. *SIAM J Sci Comput.* 1984;5(3):735–743.
- 844 77. Carvalho CM, Polson NG, Scott JG. The horseshoe estimator for sparse signals. *Biometrika.*
845 2010;97(2):465–480.
- 846 78. Dempster AP, Laird NM, Rubin DB. Maximum likelihood from incomplete data via the EM
847 algorithm. *J R Stat Soc Series B Stat Methodol.* 1977;39(1):1–22.
- 848 79. Benaglia T, Chauveau D, Hunter D, Young D. Mixtools: an R package for analyzing finite mixture
849 models. *J Stat Softw.* 2009;32(6):1–29.
- 850 80. McLachlan GJ, Lee SX, Rathnayake SI. Finite mixture models. *Annual Review of Statis-*
851 *tics and Its Application.* 2019;6(1):355–378. Available from: [https://doi.org/10.1146/](https://doi.org/10.1146/annurev-statistics-031017-100325)
852 [annurev-statistics-031017-100325](https://doi.org/10.1146/annurev-statistics-031017-100325).
- 853 81. Scrucca L, Fop M, Murphy TB, Raftery AE. mclust 5: Clustering, Classification and Density
854 Estimation Using Gaussian Finite Mixture Models. *R J.* 2016;8(1):289–317. Available from:
855 <https://www.ncbi.nlm.nih.gov/pubmed/27818791>.
- 856 82. Schwarz G. Estimating the Dimension of a Model. *Ann Statist.* 1978;6(2):461–464. Available
857 from: <https://projecteuclid.org:443/euclid.aos/1176344136>.
- 858 83. Zhou X. A unified framework for variance component estimation with summary statistics in
859 genome-wide association studies. *Ann Appl Stat.* 2017;11(4):2027–2051. Available from: <https://projecteuclid.org:443/euclid.aoas/1514430276>.
860
- 861 84. Crawford L, Zeng P, Mukherjee S, Zhou X. Detecting epistasis with the marginal epistasis test
862 in genetic mapping studies of quantitative traits. *PLoS Genet.* 2017;13(7):e1006869. Available
863 from: <https://doi.org/10.1371/journal.pgen.1006869>.
- 864 85. Chen Z, Lin T, Wang K. A powerful variant-set association test based on chi-square distribution.
865 *Genetics.* 2017;207(3):903–910.
- 866 86. Zhongxue C, Yan L, Tong L, Qingzhong L, Kai W. Gene-based genetic association test with
867 adaptive optimal weights. *Genet Epidemiol.* 2017;42(1):95–103. Available from: <https://doi.org/10.1002/gepi.22098>.
868
- 869 87. Friedman J, Hastie T, Tibshirani R. Regularization paths for generalized linear models via coor-
870 dinate descent. *J Stat Softw.* 2010;33(1):1.
- 871 88. Zeng Y, Breheny P. The biglasso package: a memory-and computation-efficient solver for lasso
872 model fitting with big data in R. *arXiv.* 2017;p. 1701.05936.

- 873 89. Duchesne P, Lafaye De Micheaux P. Computing the distribution of quadratic forms: Further
874 comparisons between the Liu–Tang–Zhang approximation and exact methods. *Comput Stat Data*
875 *Anal.* 2010;54(4):858–862. Available from: [http://www.sciencedirect.com/science/article/](http://www.sciencedirect.com/science/article/pii/S0167947309004381)
876 [pii/S0167947309004381](http://www.sciencedirect.com/science/article/pii/S0167947309004381).
- 877 90. Qayyum R, Snively BM, Ziv E, Nalls MA, Liu Y, Tang W, et al. A meta-analysis and genome-
878 wide association study of platelet count and mean platelet volume in african americans. *PLoS*
879 *Genet.* 2012;8(3):e1002491.
- 880 91. Kuleshov MV, Jones MR, Rouillard AD, Fernandez NF, Duan Q, Wang Z, et al. Enrichr:
881 a comprehensive gene set enrichment analysis web server 2016 update. *Nucleic Acids Res.*
882 2016;44(W1):W90–W97. Available from: <https://www.ncbi.nlm.nih.gov/pubmed/27141961>.
- 883 92. Lentaigne C, Freson K, Laffan MA, Turro E, Ouwehand WH, Consortium BB, et al. Inherited
884 platelet disorders: toward DNA-based diagnosis. *Blood.* 2016;127(23):2814–2823. Available from:
885 <https://www.ncbi.nlm.nih.gov/pubmed/27095789>.
- 886 93. Mousas A, Ntritsos G, Chen MH, Song C, Huffman JE, Tzoulaki I, et al. Rare coding vari-
887 ants pinpoint genes that control human hematological traits. *PLoS Genet.* 2017;13(8):e1006925–.
888 Available from: <https://doi.org/10.1371/journal.pgen.1006925>.
- 889 94. Gibson WT, Hood RL, Zhan SH, Bulman DE, Fejes AP, Moore R, et al. Mutations in *EZH2*
890 cause Weaver syndrome. *Am J Hum Genet.* 2012;90(1):110–118. Available from: [https://www.](https://www.cell.com/ajhg/fulltext/S0002-9297(11)00496-4)
891 [cell.com/ajhg/fulltext/S0002-9297\(11\)00496-4](https://www.cell.com/ajhg/fulltext/S0002-9297(11)00496-4).
- 892 95. Minczuk M, He J, Duch AM, Etema TJ, Chlebowski A, Dzionek K, et al. *TEFM* (*c17orf42*) is
893 necessary for transcription of human mtDNA. *Nucleic Acids Res.* 2011;39(10):4284–4299. Avail-
894 able from: <https://www.ncbi.nlm.nih.gov/pubmed/21278163>.
- 895 96. Carel JC, Lahlou N, Roger M, Chaussain JL. Precocious puberty and statural growth. *Hum*
896 *Reprod.* 2004;10(2):135–147. Available from: [https://academic.oup.com/humupd/article/10/](https://academic.oup.com/humupd/article/10/2/135/617162)
897 [2/135/617162](https://academic.oup.com/humupd/article/10/2/135/617162).
- 898 97. Gong J, Schumacher F, Lim U, Hindorff LA, Haessler J, Buyske S, et al. Fine Mapping and
899 Identification of BMI Loci in African Americans. *Am J Hum Genet.* 2013;93(4):661–671.
- 900 98. Locke AE, Kahali B, Berndt SI, Justice AE, Pers TH, Day FR, et al. Genetic studies of body
901 mass index yield new insights for obesity biology. *Nature.* 2015;518(7538):197–206. Available
902 from: <https://www.ncbi.nlm.nih.gov/pubmed/25673413>.
- 903 99. Dickinson ME, Flenniken AM, Ji X, Teboul L, Wong MD, White JK, et al. High-throughput
904 discovery of novel developmental phenotypes. *Nature.* 2016;537:508–514. Available from: [https:](https://doi.org/10.1038/nature19356)
905 [//doi.org/10.1038/nature19356](https://doi.org/10.1038/nature19356).
- 906 100. Baranski TJ, Kraja AT, Fink JL, Feitosa M, Lenzini PA, Borecki IB, et al. A high throughput,
907 functional screen of human Body Mass Index GWAS loci using tissue-specific RNAi *Drosophila*
908 *melanogaster* crosses. *PLoS Genet.* 2018;14(4):e1007222–. Available from: [https://doi.org/](https://doi.org/10.1371/journal.pgen.1007222)
909 [10.1371/journal.pgen.1007222](https://doi.org/10.1371/journal.pgen.1007222).
- 910 101. Safran M, Dalah I, Alexander J, Rosen N, Iny Stein T, Shmoish M, et al. GeneCards Version 3:
911 the human gene integrator. *Database.* 2010;2010. Available from: [https://academic.oup.com/](https://academic.oup.com/database/article/doi/10.1093/database/baq020/407450)
912 [database/article/doi/10.1093/database/baq020/407450](https://academic.oup.com/database/article/doi/10.1093/database/baq020/407450).

- 913 102. Vuillaume ML, Naudion S, Banneau G, Diene G, Cartault A, Cailley D, et al. New candidate
914 loci identified by array-CGH in a cohort of 100 children presenting with syndromic obesity. *Am J*
915 *Med Genet.* 2014;164(8):1965–1975. Available from: [https://onlinelibrary.wiley.com/doi/](https://onlinelibrary.wiley.com/doi/abs/10.1002/ajmg.a.36587)
916 [abs/10.1002/ajmg.a.36587](https://onlinelibrary.wiley.com/doi/abs/10.1002/ajmg.a.36587).
- 917 103. Wheeler E, Leong A, Liu CT, Hivert MF, Strawbridge RJ, Podmore C, et al. Impact of common
918 genetic determinants of Hemoglobin A1c on type 2 diabetes risk and diagnosis in ancestrally
919 diverse populations: A transethnic genome-wide meta-analysis. *PLoS Med.* 2017;14(9):e1002383.
920 Available from: [https://journals.plos.org/plosmedicine/article?id=10.1371/journal.](https://journals.plos.org/plosmedicine/article?id=10.1371/journal.pmed.1002383)
921 [pmed.1002383](https://journals.plos.org/plosmedicine/article?id=10.1371/journal.pmed.1002383).
- 922 104. Linder S, Nelson D, Weiss M, Aepfelbacher M. Wiskott-Aldrich syndrome protein regulates
923 podosomes in primary human macrophages. *Proc Natl Acad Sci U S A.* 1999;96(17):9648–9653.
924 Available from: <http://www.pnas.org/content/96/17/9648.abstract>.
- 925 105. Steele BM, Harper MT, Macaulay IC, Morrell CN, Perez-Tamayo A, Foy M, et al. Canonical Wnt
926 signaling negatively regulates platelet function. *Proc Natl Acad Sci U S A.* 2009;106(47):19836–
927 19841.
- 928 106. Macaulay IC, Thon JN, Tijssen MR, Steele BM, MacDonald BT, Meade G, et al. Canonical
929 Wnt signaling in megakaryocytes regulates proplatelet formation. *Blood.* 2013;121(1):188–196.
930 Available from: <http://www.bloodjournal.org/content/121/1/188>.
- 931 107. Stocks T, Angquist L, Hager J, Charon C, Holst C, Martinez JA, et al. TFAP2B-dietary protein
932 and glycemic index interactions and weight maintenance after weight loss in the DiOGenes trial.
933 *Hum Hered.* 2013;75(2-4):213–219.
- 934 108. Xiang J, Yang S, Xin N, Gaertig MA, Reeves RH, Li S, et al. DYRK1A regulates Hap1–
935 Dcaf7/WDR68 binding with implication for delayed growth in down syndrome. *Proc Natl Acad*
936 *Sci U S A.* 2017;114(7):E1224–E1233. Available from: [https://www.pnas.org/content/114/7/](https://www.pnas.org/content/114/7/E1224)
937 [E1224](https://www.pnas.org/content/114/7/E1224).
- 938 109. Smith CM, Finger JH, Hayamizu TF, McCright IJ, Eppig JT, Kadin JA, et al. The mouse gene
939 expression database (GXD): 2007 update. *Nucleic Acids Res.* 2006;35:D618–D623. Available
940 from: https://academic.oup.com/nar/article/35/suppl_1/D618/1085755.
- 941 110. Bult CJ, Krupke DM, Begley DA, Richardson JE, Neuhauser SB, Sundberg JP, et al. Mouse
942 Tumor Biology (MTB): a database of mouse models for human cancer. *Nucleic Acids Res.*
943 2014;43(D1):D818–D824. Available from: [https://academic.oup.com/nar/article/43/D1/](https://academic.oup.com/nar/article/43/D1/D818/2439858)
944 [D818/2439858](https://academic.oup.com/nar/article/43/D1/D818/2439858).
- 945 111. Smith CL, Blake JA, Kadin JA, Richardson JE, Bult CJ, Group MGD. Mouse Genome Database
946 (MGD)-2018: knowledgebase for the laboratory mouse. *Nucleic Acids Res.* 2017;46(D1):D836–
947 D842. Available from: <https://academic.oup.com/nar/article/47/D1/D801/5165331>.